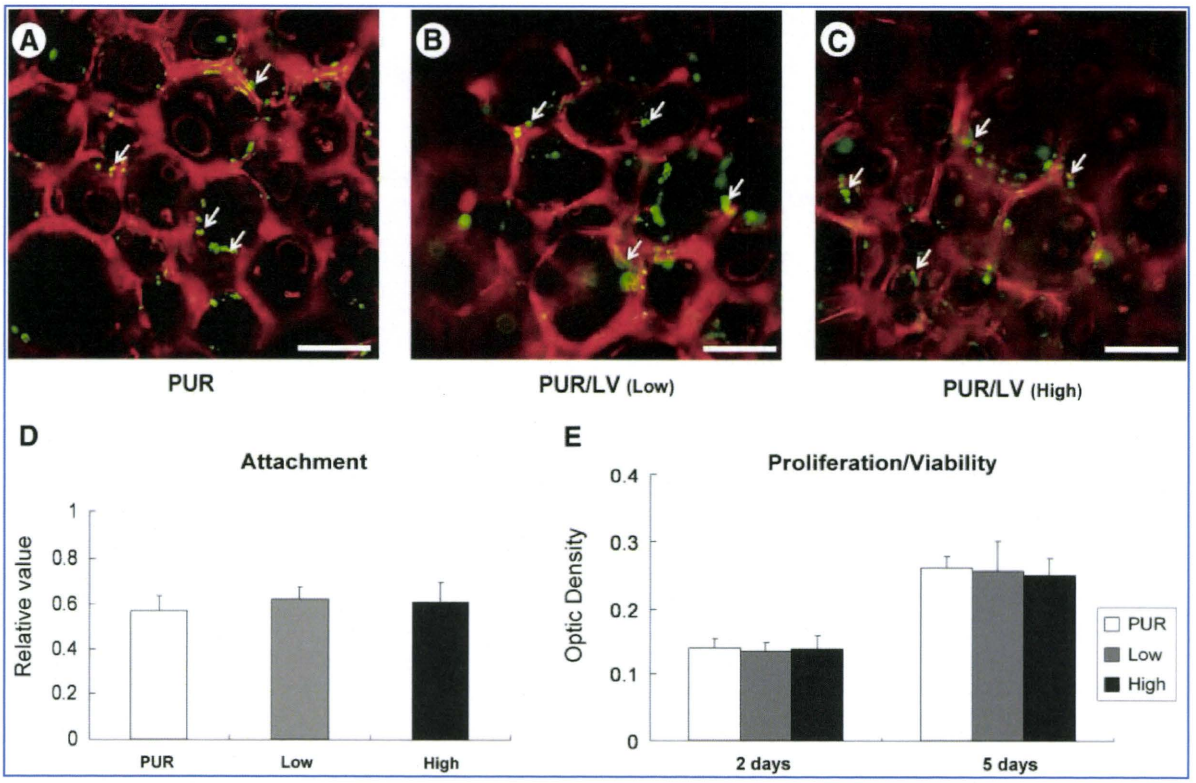

FIG. 3. *In vitro* biocompatibility of PUR/LV scaffolds. Calcein staining of viable MC3T3-E1 osteoblastic cells (green) cultured on PUR scaffolds: (**A**) PUR, (**B**) PUR/LV (Low), and (**C**) PUR/LV (High) at day 5. The arrows indicate the osteoblastic cells. Scale bars: 200 μm. Cell attachment at 4 h (**D**) and proliferation/viability at days 2 and 5 (**E**) were accessed using MTT assay ($n = 4$). Color images available online at www.liebertonline.com/ten.

BMP2 expression in the osteoblastic cells treated with LV releasates was twofold higher than that in the control. LV released from PUR scaffolds enhanced osteogenic differentiation as evidenced by ALP activity, especially at day 7 (Fig. 4B). Bone nodule formation in the cells treated with LV releasates for 25 days was also significantly enhanced when compared to the control (Fig. 4C, D). While *BMP2* gene expression, *ALP* expression, and bone nodule formation were somewhat higher for fresh LV (positive control) compared to released LV, the differences were not statistically significant, which suggests that the stimulatory potential of LV on osteogenic differentiation was preserved during the chemical reaction associated with the foaming process.

Effect of local LV delivery from PUR scaffolds on in vivo *bone formation*

To evaluate the effect of local LV delivery from PUR scaffolds on *in vivo* bone formation, cylindrical PUR scaffolds were implanted into rat femoral plug defects. At week 2, μCT analysis, which measures the amount of mineralized bone formation, showed that new bone started forming mainly at the peripheral area in the materials (Fig. 5A). There were no significant differences among the groups in the amount of new bone area and bone density (Fig. 5B, C). At week 4, μCT images showed that increased bone formation was visible throughout the implants in all treatment groups (Fig. 5A). The most extensive bone formation was observed in LV-H samples. The quantitative μCT analysis at week 4 demonstrated that the volume of new bone formation per total scaffold volume was higher in LV-H samples, although the differences were not significant ($p = 0.068$) (Fig. 5B). The density of newly formed bone in LV-H samples was significantly higher than that observed in the control PUR scaffolds at 4 weeks (Fig. 5C).

In the histological analysis, substantial cellular infiltration was observed in all groups at week 2, and new bone formation started mainly near the bottom surface of the implant (Fig. 6A). At week 4, an increased amount of mature bone formation was observed throughout the entire area of the implants (Fig. 6B). New bone formation in the scaffold was most extensive in the LV-H materials (Fig. 6C), which is consistent with the μCT analysis. The implants at week 4 had more extensively degraded in all treatment groups when compared to the samples at week 2. Although histomorphometric analysis showed no differences among groups in the area of new bone formation at week 2, LV-H samples showed significantly greater bone formation at week 4 than the control group (Fig. 6D). A significant difference in new bone formation was measured at 4 weeks for the LV-H treatment group by histomorphometry, but not by μCT. This difference in outcomes between the two experimental

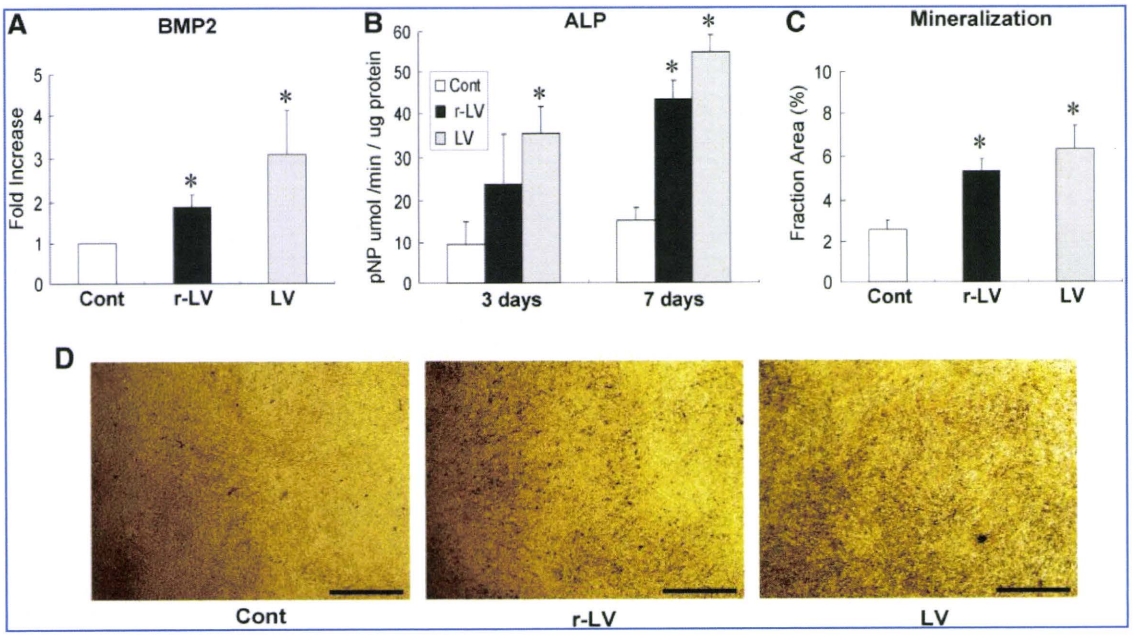

FIG. 4. Effect of LV delivery on osteogenic differentiation *in vitro*. MC3T3-E1 osteoblastic cells were treated with LV releasates from PUR scaffolds (r-LV). Fresh LV was used as a positive control (LV). (**A**) Bone morphogenetic protein 2 (BMP2) expression, (**B**) alkaline phosphatase activity (ALP) activity, and (**C, D**) mineralized nodule formation (Von Kossa staining) were evaluated ($n = 4$). Scale bars: 1 mm. $^*p < 0.05$ versus control. Color images available online at www.liebertonline.com/ten.

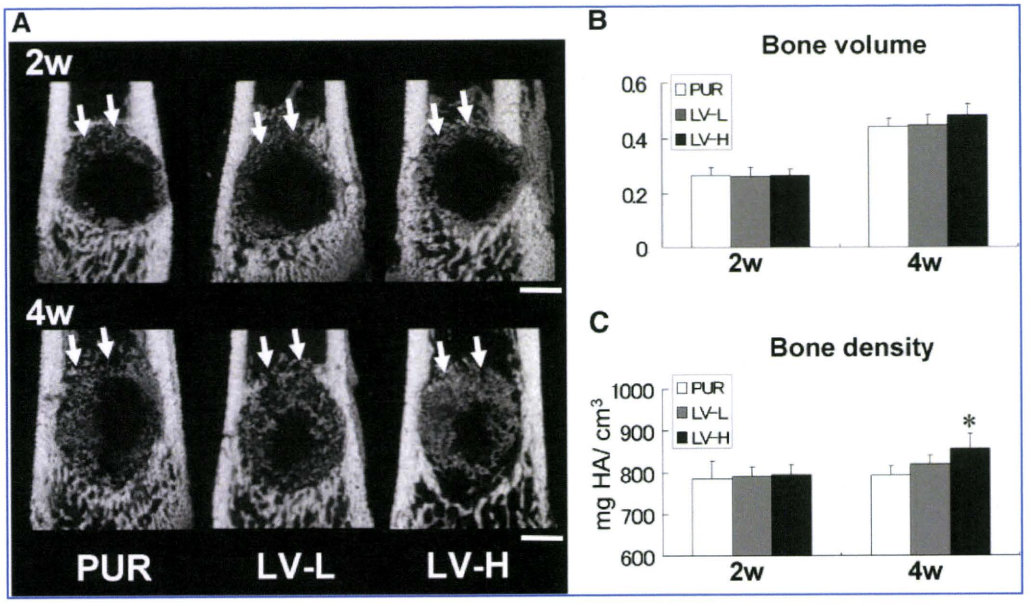

FIG. 5. Effect of local LV delivery from PUR scaffolds on *in vivo* bone formation. The PUR and PUR/LV scaffolds were implanted into rat femoral plug defects: (**A**) representative sagittal μCT images at 2 and 4 weeks postimplantation. Arrows highlight areas of new bone formation. Scale bars: 1 mm. Quantitative analysis of mineralized new bone formation: (**B**) bone volume per total volume of implants and (**C**) mean bone density ($n = 6$). $^*p < 0.05$ versus PUR.

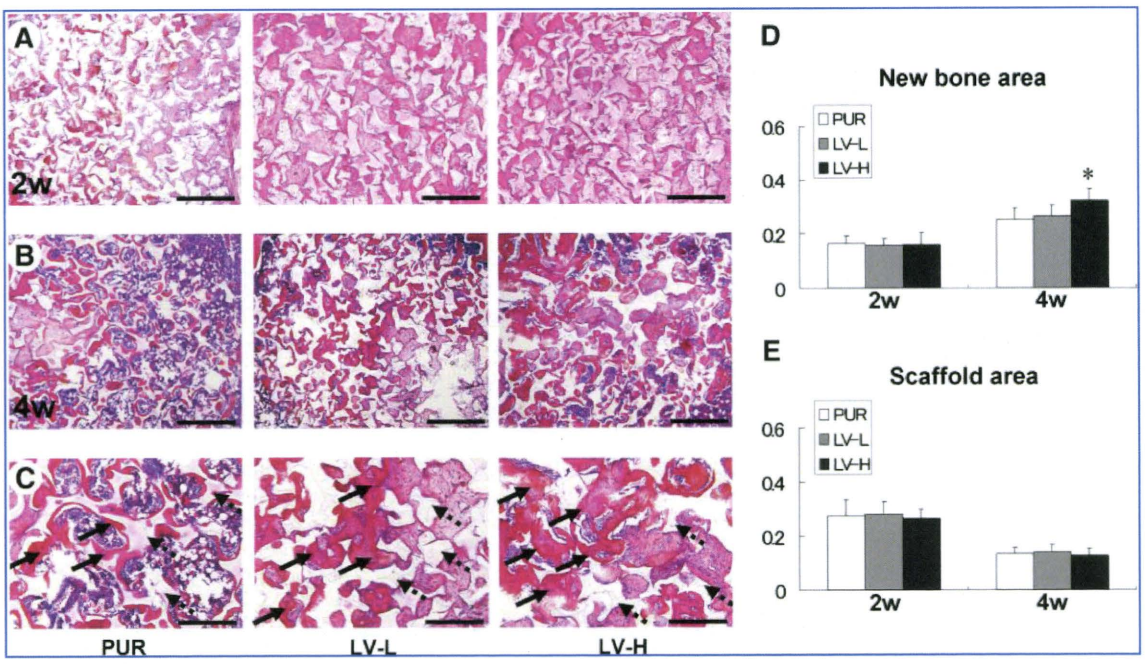

FIG. 6. Histological evaluation of *in vivo* bone formation study. Representative decalcified histological sections (hematoxylin and eosin) at (**A**) 2 weeks and (**B**) 4 weeks postimplantation (coronal). Scale bars: 1 mm. (**C**) High magnification of the sections at 4 weeks. Solid arrows indicate newly formed bone and dotted arrows indicate residual scaffolds. Scale bars: 250 μm. The area of (**D**) new bone formation and (**E**) scaffolds in the histological sections was evaluated ($n = 6$). $^*p < 0.05$ versus PUR. Color images available online at www.liebertonline.com/ten.

techniques could be attributed to the fact that the histomorphometric analysis includes both mineralized bone as well as bone matrix that is not fully mineralized, whereas the μCT analysis includes only mineralized bone. In all groups, the residual scaffold area at week 4 was nearly half that of the samples at week 2; there were no significant differences among treatment groups both at weeks 2 and 4 (Fig. 6E).

Discussion

Biodegradable PUR materials have been investigated in tissue engineering as supportive scaffolds for cell attachment, growth, and differentiation. Recent studies have shown that scaffolds fabricated from biodegradable segmented PUR elastomers comprising hexamethylene diisocyanate supported infiltration of cells and bone ingrowth when implanted in defects in the iliac crest of sheep.[12,44] Similarly, two-component lysine diisocyanate-based PUR biomaterials incorporating β-tricalcium phosphate showed bone ingrowth in femoral defects in sheep.[13] In this study, we used a high-porosity LTI-based PUR scaffold with resilient elastomeric mechanical properties.[9] The material has an ellipsoidal pore structure with interconnected pores, which supported cell attachment and growth in osteoblastic cell culture *in vitro*. In a previously reported cell culture study, MC3T3 cells were observed to migrate into the interior of the PUR scaffolds for up to 21 days, suggesting that the pores were interconnected.[15] In this *in vivo* study, cellular infiltration and ingrowth of new bone into the materials were observed as early as 2 weeks, with increased new bone formation at 4 weeks. These results suggest that the LTI-based two-component PUR scaffolds exhibit interconnected pores and demonstrate osteoconductive properties, which is in agreement with previous studies.

Since the original report describing the effects of statins in bone,[22] there have been multiple publications confirming the effects of these drugs in bone cells and many other studies looking at their mechanism of action. Statins known to inhibit the mevalonate pathway induce *BMP2* gene expression, which in turn initiates a cascade of events that ultimately stimulates osteoblasts. *BMP2* is one of the most potent osteoinductive agents involved in recruitment, proliferation, and differentiation of osteoprogenitor cells, resulting in bone formation. Considering that statins are rapidly absorbed after oral administration and their systemic bioavailability is low,[27] administering these drugs locally to defect sites was anticipated to be a more effective strategy for bone regeneration than systemic delivery.

It is intriguing that statins, drugs that are believed to primarily stimulate osteoblastic bone formation, and bisphosphonates, compounds that are well-established inhibitors of osteoclastic bone resorption, have targets in the same metabolic pathway, the mevalonate pathway of cholesterol biosynthesis. Although some studies (including the original publication) have shown statins to also affect osteoclastic bone resorption, the major effect of statins is bone formation. The actions of statins in bone can be abolished when noggin, a naturally occurring inhibitor of BMP2, is added to bone cells. It has also been demonstrated that bone formation *in vivo* is impaired in transgenic mice that have a truncated

dominant-negative type receptor (BMPR-IB) targeted to osteoblasts,[45] confirming again the importance of BMP2 as a mediator of the statin effect in bone formation. On the other hand, bisphosphonates are strong bone resorption inhibitors, although recently they have also been shown to stimulate osteoblastic bone formation.[46–48]

The fact that both statins and bisphosphonates have targets in the same metabolic pathway results in concerns regarding complications due to potential interactions between the two drugs. However, although both drug classes prevent the prenylation of guanosine triphosphate (GTP)-binding proteins, the pharmacological mechanism of action in aminobisphosphonates is based on interference with the mevalonate pathway by inhibiting the more downstream farnesyl pyrophosphate synthase enzyme, while statins act far upstream on the mevalonate pathway by inhibiting the HMG-CoA reductase. Therefore, these two drug classes interfere with distinct pathways branching from the main mevalonate pathway, and are linked to the different levels of the mevalonate pathway. Moreover, bisphosphonates preferentially bind to the surface of bone at sites of active remodeling and become internalized into osteoclasts via endocytosis, which might explain why their effects on the mevalonate pathway are much more apparent in osteoclasts. Further, bisphosphonates have been shown recently to induce formation of a novel ATP analog (Apppl) as a consequence of inhibition of the mevalonate pathway and this molecule has been shown to cause apoptosis in osteoclasts.[48] Since statins inhibit this pathway far upstream, the levels of Apppl are decreased, which might explain the different effects of both drugs. Local delivery of statins in patients taking bisphosphonates is thus not anticipated to have a detrimental effect or cause bisphosphonate-associated osteonecrosis for the above-mentioned differences in the mechanism of action. However, more detailed studies are required to determine any potential interactions between statins and bisphosphonates.

Local drug delivery achieved through incorporation of signaling molecules in a scaffold is an established and effective approach to regenerating tissue.[49,50] PUR scaffolds have been shown to deliver basic fibroblast growth factor,[17] rhPDGF-BB,[8] and rhBMP2.[18] In this study, we incorporated LV into PUR scaffolds for local delivery to bony sites by mixing it in powder form with the polyol-based hardener component before polymerization with LTI. We have previously shown that the biological activity of molecules that have active hydrogen (e.g., hydroxyl and amine) groups, such as tobramycin and PDGF, was not adversely affected by the PUR reaction when incorporated as solid particles.[8,51] In contrast, when a molecule with active hydrogen groups was added to the two-component formulation as an aqueous solution, the release was almost negligible due to covalent bonding between the bioactive molecule and the PUR.[51] The encapsulation of LV particles did not noticeably affect the morphology of the PUR scaffolds, as shown by SEM analysis. The highly porous structure with interconnected pores, which supported cell attachment and growth, was preserved well in the PUR scaffolds even with LV incorporation. As a result, PUR/LV scaffolds demonstrated equal potential for osteoblastic cell attachment and proliferation *in vitro* as PUR scaffolds without LV. PUR/LV and PUR scaffolds also showed similar abilities to allow cell infiltration to the scaffolds *in vivo* at 2 weeks postimplantation.

To deliver statins safely and effectively to the wound site, a sustained local delivery system is preferred to systemic delivery. An initial burst release of statins raises cytotoxicity concerns due to the dramatically reduced production of cholesterol, a molecule required for membrane integrity. Further, an adverse inflammatory response has been reported after local administration of high doses of statins *in vivo*.[33,34] In the present study, LV release from PUR scaffolds followed a sustained and linear profile, thus minimizing the potentially negative side effects of locally high statin concentrations. The burst release was <3%, and after the 30 days the cumulative release varied from 12% to 22%. These data are in agreement with a previous study investigating the release of simvastatin (which also has very low water solubility) from poly(lactic-*co*-glycolic acid) (PLGA) scaffolds, where the burst release was 5% and the cumulative release at 30 days was 32%.[35] Release of LV particles from PUR scaffolds is thus conjectured to be diffusion-controlled, as reported previously for simvastatin particles embedded in PLGA scaffolds. Due in part to the low water solubility of LV (0.4 μg/mL), the diffusion-controlled release occurs slowly, and under *in vitro* conditions is primarily independent of PUR degradation, considering that the degradation time of these materials is on the order of weeks to months.[51] The higher cumulative release of LV observed at the high dose relative to the low dose (Fig. 1C) is conjectured to result from the formation of channels created by LV, which has already diffused away from the interior of the scaffold.[52] Thus, a higher LV loading is anticipated to create more (or larger) channels for LV diffusion from the polymer, resulting in accelerated release kinetics. Previously, we have shown that a hydrophilic drug with high water solubility, such as tobramycin, is released much faster from PUR scaffolds with an initial burst release >30%.[51] The release rate can be accelerated slightly by incorporating PEG, which increases the hydrophilicity and swelling of the PUR scaffold (LV data not shown).[51] Faster release rates of statins have been achieved through other approaches, such as encapsulation of LV in nanospheres 50–350 nm in diameter, which exhibited a minimal burst release and 25% cumulative release after 10 days, presumably due to the relatively short diffusion path.[37] While encapsulation of LV in 50–350 nm nanoparticles has been shown to achieve more efficient release kinetics, we have previously shown that incorporation of ~1 μm microspheres in a PUR scaffold substantially reduced the rate of release relative to the microspheres alone. In contrast, scaffolds incorporating ~100 μm microspheres exhibited release kinetics comparable to that of the microspheres alone.[18] This reduction in release kinetics observed for small (<1 μm) particles embedded in the scaffolds was attributed to the increased resistance to mass transfer resulting from the pore walls. In another study, fluvastatin (which has substantially higher water solubility than LV) tethered to a PEG hydrogel by a degradable lactic acid spacer–exhibited tunable release kinetics, with 100% cumulative release after 7–40 days *in vitro*.[36] The faster release kinetics observed for the fluvastatin hydrogel delivery system is attributed to the degradation-controlled release mechanism in contrast to the diffusion-controlled mechanism associated with the PUR scaffolds.

The scaffolds both with and without LV exhibited biocompatibility when cultured with osteoblastic cells *in vitro*.

While the PUR scaffolds were not directly compared to other materials in this study, previous studies have shown that the lysine polyisocyanate-derived PUR scaffolds support cellular attachment and proliferation comparably to other polymeric biomaterials, including tissue culture polystyrene, PLGA, and polyethylene for periods up to 21 days.[14,15] Histological analysis demonstrated substantial degradation of PUR scaffolds at week 4 *in vivo*, which is in agreement with previous studies demonstrating the PUR scaffolds degrade to non-cytotoxic decomposition products.[9,53] None of the histological sections showed severe inflammation, suggesting that neither the PUR degradation products nor the released LV induced an adverse inflammatory response for the LV doses used in this study. In a previous study, rats treated with simvastatin in a methylcellulose gel on the lateral aspect of the mandible exhibited 45% more bone formation and reduced clinical swelling when the simvastatin dose was reduced from 2.2 mg to 500 μg.[33] These facts suggest that the PUR/LV sustained delivery system can be used safely for bone tissue repair by delivering LV doses that are high enough to promote new bone formation but below the threshold for inflammation.

On the basis of the fact that LV needs to be converted to the hydrophilic acid form to become biologically active,[54] we examined the effect of LV released from PUR scaffolds on osteogenesis *in vitro* to verify the bioactivity of the released compounds. These experiments were designed to determine whether the biological activity of LV was adversely affected by the PUR reaction. Induction of osteogenic differentiation and mineralization, as evaluated by ALP activity and mineralized nodule formation, resulted when MC3T3-E1 osteoblastic cells were cultured with LV releaseates. Osteogenic differentiation in MC3T3-E1 osteoblastic cells is promoted by simvastatin through increased BMP2 expression.[24,25] Similarly, the enhanced ALP activity and mineralized nodule formation in this study is attributed to increased expression of BMP2 caused by LV releasates, suggesting that LV is released from PUR scaffolds in an active form and the stimulatory osteogenic effect by promoting BMP2 production is thus preserved. Since the osteogenic potential of BMP2 is well known to be beneficial for fracture repair and regenerating bone defects,[55–57] delivery of bioactive LV with PUR scaffolds can be useful for bone regeneration.

In clinical settings, defects in long bone caused by pathological or traumatic conditions (e.g., bone tumors, infections, or major trauma) often require reconstruction using bone substitutes.[58] To evaluate the anabolic effect of LV in long bone defects and investigate its utility as a bone void filler, the PUR/LV scaffolds were evaluated in a rat femoral defect model, which is highly reproducible and useful for investigating the efficacy of new materials and drugs.[18] While published reports have demonstrated the efficacy of LV for healing of fractures and defects in craniofacial bone, the effects of local delivery of LV on healing of orthopedic long bone defects are not known. We therefore reasoned that the femoral plug model was an appropriate starting point before testing the materials in more challenging critical-sized defects. The *in vivo* study demonstrated that new bone formation was enhanced by local delivery of LV from PUR scaffolds, which is consistent with several previous studies for bone defect repair using statins.[34,59,60] The biological activity of statins *in vivo* is attributed to increased production of endogenous BMP2.[61] Interestingly, there were no differences in the amount of bone formation at week 2, which contrasts with previous studies reporting new bone formation as early as day 5 in rabbit parietal bone defects treated with simvastatin delivered from a collagen sponge.[59,60] However, bone matrix formation observed in histological sections was significantly promoted by local delivery of LV at week 4. Although the difference in mineralized bone volume evaluated by μCT was not statistically significant at week 4, it is possible that the effects of LV on mineralized bone formation may extend beyond week 4. It is known that progenitor cells require time to substantially infiltrate the defect and scaffold.[62] Therefore, the effect of LV in enhancing endogenous BMP2 production may be delayed until these cells are present, at which point subsequent osteogenic differentiation and mineralization can occur. For this reason, a sustained statin release profile may be important, considering that statins could be most effective when a substantial number of cells have migrated into the scaffolds rather than during the initial few days after surgery. In our previous fracture healing study using LV, delayed percutaneous injection of LV (1 week after surgery) into the fracture site resulted in enhanced fracture repair relative to injection within 1 day in a rat model.[63] The improvement in repair associated with delayed injection was considered to result from a larger number of cells at the fracture site. In another study, simvastatin released from a calcium sulfate carrier did not enhance new bone formation at 2 and 4 weeks in critical-sized calvarial defects in rats.[34] However, at 8 weeks, the simvastatin-treated defects exhibited significantly more new bone formation relative to the calcium sulfate controls. These observations further suggest that sustained release of LV from scaffolds is important for effective bone formation.

In the non-critical-sized plug defect model used in this study, a faster release profile of an anabolic drug would likely perform better than a slower release profile for the necessarily short observation periods due to the fast healing of the defect.[18] Therefore, a larger defect model, such as a critical-sized segmental defect,[64,65] could be more suitable for longer observation periods, and thus should be considered for further examination to investigate the effects of sustained release of LV on bone formation.

Conclusions

In this study, we investigated the effects of local delivery of LV from PUR scaffolds on osteoblastic differentiation *in vitro* and new bone formation *in vivo*. At a dose of 200 μg, the LV concentration was sufficiently high to enhance new bone formation in a rat femoral plug model, but below the threshold at which adverse inflammation occurs. Further studies are required to investigate the effects of local delivery of LV on healing of more challenging wounds, such as critical-size defects. However, this study showed the potential of using statins to enhance healing of bony defects through local delivery from polymeric scaffolds.

Acknowledgments

This work was supported by the USAISR Orthopaedic Trauma Research Program and Vanderbilt University School of Engineering. The authors thank Katarzyna J. Zienkiewicz for measuring LV by HPLC.

Disclosure Statement

Gregory R. Mundy and Gloria E. Gutierrez have stock options in OsteoGenix, which own issued patents on the effects of statins on bone. None of the other authors have conflict of interests.

References

1. Lysaght, M.J., and Reyes, J. The growth of tissue engineering. Tissue Eng **7,** 485, 2001.
2. Enneking, W.F., Eady, J.L., and Burchardt, H. Autogenous cortical bone grafts in the reconstruction of segmental skeletal defects. J Bone Joint Surg Am **62,** 1039, 1980.
3. Younger, E.M., and Chapman, M.W. Morbidity at bone graft donor sites. J Orthop Trauma **3,** 192, 1989.
4. Perry, C.R. Bone repair techniques, bone graft, and bone graft substitutes. Clin Orthop Relat Res **360,** 71, 1999.
5. Finkemeier, C.G. Bone-grafting and bone-graft substitutes. J Bone Joint Surg Am **84-A,** 454, 2002.
6. Giannoudis, P.V., Dinopoulos, H., and Tsiridis, E. Bone substitutes: an update. Injury **36 Suppl 3,** S20, 2005.
7. Zhang, J.Y., Beckman, E.J., Hu, J., Yang, G.G., Agarwal, S., and Hollinger, J.O. Synthesis, biodegradability, and biocompatibility of lysine diisocyanate-glucose polymers. Tissue Eng **8,** 771, 2002.
8. Li, B., Davidson, J.M., and Guelcher, S.A. The effect of the local delivery of platelet-derived growth factor from reactive two-component polyurethane scaffolds on the healing in rat skin excisional wounds. Biomaterials **30,** 3486, 2009.
9. Hafeman, A.E., Li, B., Yoshii, T., Zienkiewicz, K., Davidson, J.M., and Guelcher, S.A. Injectable biodegradable polyurethane scaffolds with release of platelet-derived growth factor for tissue repair and regeneration. Pharm Res **25,** 2387, 2008.
10. Guan, J., Sacks, M.S., Beckman, E.J., and Wagner, W.R. Synthesis, characterization, and cytocompatibility of elastomeric, biodegradable poly(ester-urethane)ureas based on poly(caprolactone) and putrescine. J Biomed Mater Res **61,** 493, 2002.
11. Fujimoto, K.L., Guan, J., Oshima, H., Sakai, T., and Wagner, W.R. *In vivo* evaluation of a porous, elastic, biodegradable patch for reconstructive cardiac procedures. Ann Thorac Surg **83,** 648, 2007.
12. Gorna, K., and Gogolewski, S. Preparation, degradation, and calcification of biodegradable polyurethane foams for bone graft substitutes. J Biomed Mater Res A **67,** 813, 2003.
13. Adhikari, R., Gunatillake, P.A., Griffiths, I., Tatai, L., Wickramaratna, M., Houshyar, S., *et al.* Biodegradable injectable polyurethanes: synthesis and evaluation for orthopaedic applications. Biomaterials **29,** 3762, 2008.
14. Guelcher, S.A., Patel, V., Gallagher, K.M., Connolly, S., Didier, J.E., Doctor, J.S., and Hollinger, J.O. Synthesis and *in vitro* biocompatibility of injectable polyurethane foam scaffolds. Tissue Eng **12,** 1247, 2006.
15. Guelcher, S., Srinivasan, A., Hafeman, A., Gallagher, K., Doctor, J., Khetan, S., McBride, S., and Hollinger, J. Synthesis, *in vitro* degradation, and mechanical properties of two-component poly(ester urethane)urea scaffolds: effects of water and polyol composition. Tissue Eng **13,** 2321, 2007.
16. Guelcher, S.A. Biodegradable polyurethanes: synthesis and applications in regenerative medicine. Tissue Eng Part B Rev **14,** 3, 2008.
17. Guan, J., Stankus, J.J., and Wagner, W.R. Biodegradable elastomeric scaffolds with basic fibroblast growth factor release. J Control Release **120,** 70, 2007.
18. Li, B., Yoshii, T., Hafeman, A.E., Nyman, J.S., Wenke, J.C., and Guelcher, S.A. The effects of rhBMP-2 released from biodegradable polyurethane/microsphere composite scaffolds on new bone formation in rat femora. Biomaterials **30,** 6768, 2009.
19. Liao, J.K., and Laufs, U. Pleiotropic effects of statins. Annu Rev Pharmacol Toxicol **45,** 89, 2005.
20. Almuti, K., Rimawi, R., Spevack, D., and Ostfeld, R.J. Effects of statins beyond lipid lowering: potential for clinical benefits. Int J Cardiol **109,** 7, 2006.
21. Weber, M.S., Youssef, S., Dunn, S.E., Prod'homme, T., Neuhaus, O., Stuve, O., Greenwood, J., Steinman, L., and Zamvil, S.S. Statins in the treatment of central nervous system autoimmune disease. J Neuroimmunol **178,** 140, 2006.
22. Mundy, G., Garrett, R., Harris, S., Chan, J., Chen, D., Rossini, G., Boyce, B., Zhao, M., and Gutierrez, G. Stimulation of bone formation *in vitro* and in rodents by statins. Science **286,** 1946, 1999.
23. Garrett, I.R., Gutierrez, G., and Mundy, G.R. Statins and bone formation. Curr Pharm Des **7,** 715, 2001.
24. Maeda, T., Matsunuma, A., Kawane, T., and Horiuchi, N. Simvastatin promotes osteoblast differentiation and mineralization in MC3T3-E1 cells. Biochem Biophys Res Commun **280,** 874, 2001.
25. Maeda, T., Matsunuma, A., Kurahashi, I., Yanagawa, T., Yoshida, H., and Horiuchi, N. Induction of osteoblast differentiation indices by statins in MC3T3-E1 cells. J Cell Biochem **92,** 458, 2004.
26. Baek, K.H., Lee, W.Y., Oh, K.W., Tae, H.J., Lee, J.M., Lee, E.J., Han, J.H., Kang, M.I., Cha, B.Y., Lee, K.W., Son, H.Y., and Kang, S.K. The effect of simvastatin on the proliferation and differentiation of human bone marrow stromal cells. J Korean Med Sci **20,** 438, 2005.
27. Schachter, M. Chemical, pharmacokinetic and pharmacodynamic properties of statins: an update. Fundam Clin Pharmacol **19,** 117, 2005.
28. Armitage, J. The safety of statins in clinical practice. Lancet **370,** 1781, 2007.
29. Mundy, G.R. Statins and their potential for osteoporosis. Bone **29,** 495, 2001.
30. Gonyeau, M.J. Statins and osteoporosis: a clinical review. Pharmacotherapy **25,** 228, 2005.
31. Gutierrez, G.E., Lalka, D., Garrett, I.R., Rossini, G., and Mundy, G.R. Transdermal application of lovastatin to rats causes profound increases in bone formation and plasma concentrations. Osteoporos Int **17,** 1033, 2006.
32. Toh, S., and Hernandez-Diaz, S. Statins and fracture risk. A systematic review. Pharmacoepidemiol Drug Saf **16,** 627, 2007.
33. Stein, D., Lee, Y., Schmid, M.J., Killpack, B., Genrich, M.A., Narayana, N., *et al.* Local simvastatin effects on mandibular bone growth and inflammation. J Periodontol **76,** 1861, 2005.
34. Nyan, M., Sato, D., Oda, M., Machida, T., Kobayashi, H., Nakamura, T., and Kasugai, S. Bone formation with the combination of simvastatin and calcium sulfate in critical-sized rat calvarial defect. J Pharmacol Sci **104,** 384, 2007.
35. Whang, K., McDonald, J., Khan, A., and Satsangi, N. A novel osteotropic biomaterial OG-PLG: synthesis and *in vitro* release. J Biomed Mater Res A **74A,** 237, 2005.
36. Benoit, D.S., Nuttelman, C.R., Collins, S.D., and Anseth, K.S. Synthesis and characterization of a fluvastatin-releasing hydrogel delivery system to modulate hMSC differentiation and function for bone regeneration. Biomaterials **27,** 6102, 2006.

37. Garrett, I.R., Gutierrez, G.E., Rossini, G., Nyman, J., McCluskey, B., Flores, A., and Mundy, G.R. Locally delivered lovastatin nanoparticles enhance fracture healing in rats. J Orthop Res **25,** 1351, 2007.
38. Jeon, J.H., Piepgrass, W.T., Lin, Y.L., Thomas, M.V., and Puleo, D.A. Localized intermittent delivery of simvastatin hydroxyacid stimulates bone formation in rats. J Periodontol **79,** 1457, 2008.
39. Wutticharoenmongkol, P., Pavasant, P., and Supaphol, P. Osteoblastic phenotype expression of MC3T3-E1 cultured on electrospun polycaprolactone fiber mats filled with hydroxyapatite nanoparticles. Biomacromolecules **8,** 2602, 2007.
40. Zhang, L.F., Yang de, J., Chen, H.C., Sun, R., Xu, L., Xiong, Z.C., Govender, T., and Xiong, C.D. An ionically crosslinked hydrogel containing vancomycin coating on a porous scaffold for drug delivery and cell culture. Int J Pharm **353,** 74, 2008.
41. Zhao, M., Ko, S.Y., Liu, J.H., Chen, D., Zhang, J., Wang, B., Harris, S.E., Oyajobi, B.O., and Mundy, G.R. Inhibition of microtubule assembly in osteoblasts stimulates bone morphogenetic protein 2 expression and bone formation through transcription factor Gli2. Mol Cell Biol **29,** 1291, 2009.
42. Karp, J.M., Rzeszutek, K., Shoichet, M.S., and Davies, J.E. Fabrication of precise cylindrical three-dimensional tissue engineering scaffolds for *in vitro* and *in vivo* bone engineering applications. J Craniofac Surg **14,** 317, 2003.
43. Torigoe, I., Sotome, S., Tsuchiya, A., Yoshii, T., Maehara, H., Sugata, Y., Inchinose, S., Shinomiya, K., and Okawa, A. Bone regeneration with autologous plasma, bone marrow stromal cells, and porous beta-tricalcium phosphate in nonhuman primates. Tissue Eng Part A **15,** 1489, 2009.
44. Gorna, K., and Gogolewski, S. Biodegradable polyurethanes for implants. II. *In vitro* degradation and calcification of materials from poly(epsilon-caprolactone)-poly(ethylene oxide) diols and various chain extenders. J Biomed Mater Res **60,** 592, 2002.
45. Zhao, M., Harris, S.E., Horn, D., Geng, Z., Nishimura, R., Mundy, G.R., and Chen, D. Bone morphogenetic protein receptor signaling is necessary for normal murine postnatal bone formation. J Cell Biol **157,** 1049, 2002.
46. Im, G.I., Qureshi, S.A., Kenney, J., Rubash, H.E., and Shanbhag, A.S. Osteoblast proliferation and maturation by bisphosphonates. Biomaterials **25,** 4105, 2004.
47. Reinholz, G.G., Getz, B., Pederson, L., Sanders, E.S., Subramaniam, M., Ingle, J.N., and Spelsberg, T.C. Bisphosphonates directly regulate cell proliferation, differentiation, and gene expression in human osteoblasts. Cancer Res **60,** 6001, 2000.
48. Plotkin, L.I., Weinstein, R.S., Parfitt, A.M., Roberson, P.K., Manolagas, S.C., and Bellido, T. Prevention of osteocyte and osteoblast apoptosis by bisphosphonates and calcitonin. J Clin Invest **104,** 1363, 1999.
49. Rose, F.R., Hou, Q., and Oreffo, R.O. Delivery systems for bone growth factors—the new players in skeletal regeneration. J Pharm Pharmacol **56,** 415, 2004.
50. Drosse, I., Volkmer, E., Capanna, R., De Biase, P., Mutschler, W., and Schieker, M. Tissue engineering for bone defect healing: an update on a multi-component approach. Injury **39 Suppl 2,** S9, 2008.
51. Hafeman, A.E., Zienkiewicz, K.J., Carney, E., Litzner, B., Stratton, C.W., Wenke, J.C., and Guelcher, S.A. Local delivery of tobramycin from injectable biodegradable polyurethane scaffolds. J Biomater Sci Polym Ed **21,** 95, 2010.
52. Park, K. Controlled Drug Delivery: Challenges and Strategies. Washington, DC: American Chemical Society, 1997.
53. Guelcher, S.A., Dumas, J., Srinivasan, A., Didier, J.E., and Hollinger, J.O. Synthesis, mechanical properties, biocompatibility, and biodegradation of polyurethane networks from lysine polyisocyanates. Biomaterials **29,** 1762, 2008.
54. Alessandri, C., and Peverini, F. [Hypercholesterolemia: therapeutic approach]. Clin Ter **137,** 373, 1991.
55. Mont, M.A., Ragland, P.S., Biggins, B., Friedlaender, G., Patel, T., Cook, S., *et al.* Use of bone morphogenetic proteins for musculoskeletal applications. An overview. J Bone Joint Surg Am **86-A Suppl 2,** 41, 2004.
56. Wozney, J.M., and Rosen, V. Bone morphogenetic protein and bone morphogenetic protein gene family in bone formation and repair. Clin Orthop Relat Res **346,** 26, 1998.
57. Termaat, M.F., Den Boer, F.C., Bakker, F.C., Patka, P., and Haarman, H.J. Bone morphogenetic proteins. Development and clinical efficacy in the treatment of fractures and bone defects. J Bone Joint Surg Am **87,** 1367, 2005.
58. Paderni, S., Terzi, S., and Amendola, L. Major bone defect treatment with an osteoconductive bone substitute. Chir Organi Mov **93,** 89, 2009.
59. Wong, R.W., and Rabie, A.B. Statin collagen grafts used to repair defects in the parietal bone of rabbits. Br J Oral Maxillofac Surg **41,** 244, 2003.
60. Wong, R.W., and Rabie, A.B. Histologic and ultrastructural study on statin graft in rabbit skulls. J Oral Maxillofac Surg **63,** 1515, 2005.
61. Alam, S., Ueki, K., Nakagawa, K., Marukawa, K., Hashiba, Y., Yamamoto, E., Sakulsak, N., and Iseki, S. Statin-induced bone morphogenetic protein (BMP) 2 expression during bone regeneration: an immunohistochemical study. Oral Surg Oral Med Oral Pathol Oral Radiol Endod **107,** 22, 2009.
62. Seeherman, H., Li, R., Bouxsein, M., Kim, H., Li, X.J., Smith-Adaline, E.A., Aiolova, M., and Wozney, J.M. rhBMP-2/calcium phosphate matrix accelerates osteotomy-site healing in a nonhuman primate model at multiple treatment times and concentrations. J Bone Joint Surg Am **88,** 144, 2006.
63. Gutierrez, G.E., Nyman, J.S., Munoz, S., Jadhav, S., Yoshii, T., Esparza, J.M., and Mundy, G.R. Sustained release lovastatin applied one week after fracture accelerates healing in a rat model of fracture repair. Abstract presented at the 55th Orthopaedic Research Society Annual Meeting, Las Vegas, NV, 2009. Abstract no. 130.
64. Moore, D.C., Pedrozo, H.A., Crisco, J.J., 3rd, and Ehrlich, M.G. Preformed grafts of porcine small intestine submucosa (SIS) for bridging segmental bone defects. J Biomed Mater Res A **69,** 259, 2004.
65. Chu, T.M., Warden, S.J., Turner, C.H., and Stewart, R.L. Segmental bone regeneration using a load-bearing biodegradable carrier of bone morphogenetic protein-2. Biomaterials **28,** 459, 2007.

Address correspondence to:
Scott A. Guelcher, Ph.D.
Department of Chemical and Biomolecular Engineering
Vanderbilt University
2301 Vanderbilt Place
VU Station B #351604
Nashville, TN 37235

E-mail: scott.guelcher@vanderbilt.edu

Received: August 31, 2009
Accepted: March 4, 2010
Online Publication Date: April 5, 2010

ARTHRITIS & RHEUMATISM
Vol. 62, No. 5, May 2010, pp 1329–1337
DOI 10.1002/art.27400

Osteopontin Deficiency Impairs Wear Debris–Induced Osteolysis via Regulation of Cytokine Secretion From Murine Macrophages

Sadanori Shimizu,[1] Naoki Okuda,[1] Norihiko Kato,[2] Susan R. Rittling,[3] Atsushi Okawa,[2] Kenichi Shinomiya,[1] Takeshi Muneta,[1] David T. Denhardt,[3] Masaki Noda,[1] Kunikazu Tsuji,[4] and Yoshinori Asou[2]

Objective. **To investigate the molecular mechanisms underlying particle-induced osteolysis, we focused on osteopontin (OPN), a cytokine and cell-attachment protein that is associated with macrophage chemoattractant and osteoclast activation.**

Methods. **We compared OPN protein levels in human periprosthetic osteolysis tissues with those in osteoarthritis (OA) synovial tissues. To investigate the functions of OPN during particle-induced osteolysis in vivo, titanium particles were implanted onto the calvaria of OPN-deficient mice and their wild-type (WT) littermates. Mice were killed on day 10 and evaluated immunohistologically. The effects of OPN deficiency on the secretion of inflammatory cytokines were examined using cultured bone marrow–derived macrophages (BMMs). BMMs from OPN-deficient and WT mice were cultured with titanium particles for 12 hours, and the concentrations of inflammatory cytokines in the conditioned media were measured by enzyme-linked immunosorbent assay.**

Results. **Expression of OPN protein was enhanced in human periprosthetic osteolysis tissues as compared with OA synovial tissues. In the particle-induced model of osteolysis of the calvaria, bone resorption was significantly suppressed by OPN deficiency via inhibition of osteoclastogenesis, whereas an inflammatory reaction was observed regardless of the genotype. Results of immunostaining indicated that OPN protein was highly expressed in the membrane and bone surface at the area of bone resorption in WT mice. When BMMs were exposed to titanium particles, the concentration of proinflammatory cytokines, such as tumor necrosis factor α, interleukin-1α (IL-1α), IL-1β, and IL-6, as well as chemotactic factors, such as monocyte chemoattractant protein 1 and macrophage inflammatory protein 1α, in the conditioned medium were significantly reduced by OPN deficiency. Whereas phagocytic activity of BMMs was not attenuated by OPN deficiency, phagocytosis-mediated NF-κB activation was impaired in OPN-deficient BMMs. These data indicated that OPN was implicated in the development of particle-induced osteolysis via the orchestration of pro-/antiinflammatory cytokines secreted from macrophages.**

Conclusion. **OPN plays critical roles in wear debris–induced osteolysis, suggesting that OPN is a candidate therapeutic target for periprosthetic osteolysis.**

Total joint arthroplasty has been a significant advance in the treatment of osteoarthritis (OA), rheumatoid arthritis (RA), and other arthritic diseases affecting the major joints of the upper and lower extremities (1). Despite improvements in implant design and surgical techniques, periprosthetic osteolysis causing

Supported by a 21st Century Global Center of Excellence program grant.

[1]Sadanori Shimizu, MD, PhD, Naoki Okuda, MD, PhD, Kenichi Shinomiya, MD, PhD, Takeshi Muneta, MD, PhD, Masaki Noda, MD, PhD: International Research Center for Molecular Science in Tooth and Bone Diseases, and Tokyo Medical and Dental University, Tokyo, Japan; [2]Norihiko Kato, MD, PhD, Atsushi Okawa, MD, PhD, Yoshinori Asou, MD, PhD: Tokyo Medical and Dental University, Tokyo, Japan; [3]Susan R. Rittling, PhD (current address: The Forsyth Institute, Boston, Massachusetts), David T. Denhardt, PhD: Rutgers University, Piscataway, New Jersey; [4]Kunikazu Tsuji, PhD: International Research Center for Molecular Science in Tooth and Bone Diseases, Tokyo, Japan.

Address correspondence and reprint requests to Yoshinori Asou, MD, PhD, Department of Orthopedic Surgery, Tokyo Medical and Dental University, 1-5-45 Yushima, Bunkyo-ku, Tokyo 113-8519, Japan. E-mail: aso.orth@tmd.ac.jp.

Submitted for publication December 14, 2008; accepted in revised form February 4, 2010.

aseptic loosening of artificial joints remains the most serious problem limiting clinical success (2). Reaction to plastic, metal, and acrylic particles results in the formation of granulation tissue containing macrophages and giant cells (3). Periprosthetic osteolysis often occurs as a result of particle phagocytosis by macrophages, which leads to the secretion of inflammatory cytokines, such as interleukin-1 (IL-1) and IL-6, and chemokines, such as monocyte chemoattractant protein 1 (MCP-1) and macrophage inflammatory protein 1α (MIP-1α) (4–8). This process, in turn, leads to the production of the essential osteoclast differentiation factor, RANKL, by stromal cells and activated T cells. RANKL directly stimulates osteoclastogenesis and bone resorption by binding to its receptor (RANK) on osteoclast precursor cells (9–11).

Osteopontin (OPN) is localized to cell–matrix and matrix–matrix interfaces in mineralized tissues, where it is deposited as the result of osteoclast action (12). OPN expression is increased in response to early proinflammatory cytokines and to mechanical strain in bone (13). OPN binds to a subset of integrin receptors; most notably, it is a well-characterized ligand for $\alpha v\beta 3$ integrin, which is expressed at high levels in osteoclasts and endothelial cells (13,14). Therefore, OPN mediates the inflammatory process and subsequent bone resorption by osteoclasts (13). Because OPN expression is induced by many inflammatory cytokines and is produced by macrophages in response to inflammatory stimuli (12), we hypothesized that OPN might be involved in osteolysis (15,16). Indeed, OPN protein and messenger RNA (mRNA) are expressed by macrophages in periprosthetic tissue from patients with aseptically loosened prostheses (17).

To investigate the role of OPN in bone resorptive disorders, such as ovariectomy-induced bone resorption, ectopic bone resorption, and RA, OPN-deficient mice have been examined (14,18,19). Although these pathologic bone resorption conditions are impaired in OPN-deficient mice, the mice have normal skeletal size and patterning (20). In addition, osteoclasts are morphologically normal in OPN-deficient mice (21).

Since OPN is produced by synovial cells, chondrocytes, and osteoblasts, as well as by osteoclasts, this protein has been suggested to play a role in bone diseases caused by abnormal inflammation (19). However, its function in particle-induced osteolysis remains unknown. The purpose of this study was to investigate the functions of OPN in the process of periprosthetic osteolysis.

MATERIALS AND METHODS

Human periprosthetic tissue collection. Tissue samples were collected from the bone–implant interface membranes of 4 patients undergoing revision surgery for aseptic loosening of total hip replacement prosthesis. Control samples were obtained from the joint synovia of 8 patients undergoing primary total hip replacement surgery for OA. There were no clinical or radiologic signs of infection in any tissue sample analyzed.

OPN protein levels in human tissue samples. Protein from human tissue samples was extracted with the use of BioMasher (Investigen) and CelLytic MT (Sigma). Levels of OPN protein in tissue samples were quantified using a human OPN enzyme-linked immunosorbent assay (ELISA) kit according to the manufacturer's protocol (Immuno-Biological Laboratories). All ELISA results were normalized to tissue protein levels, which were quantified using a bicinchoninic acid protein assay kit (Pierce).

Animals. Wild-type (WT) and OPN-deficient mice on the (C57BL/6 $\times$ 129/Sv)F_2 background were produced as previously described (20). Female OPN-deficient mice and WT littermates (1.5–3-month-old) were used in the experiments. All animal experiments were approved by the animal welfare committee at Tokyo Medical and Dental University.

Particles. Pure titanium particles measuring 1–3 μm in diameter were obtained from Alfa Aesar (lot no. L01H16) and were prepared as previously described (22). Briefly, particles of 1–3 μm in diameter were suspended in phosphate buffered saline at a concentration of 1×10^8/ml, washed in 70% ethanol at room temperature, and dried on a clean bench under ultraviolet radiation.

In vivo mouse calvaria resorption model. Eight healthy female OPN-deficient mice and 9 healthy female WT littermates were anesthetized, and their scalps were incised longitudinally to expose the external cranial periosteum. The periosteum was elevated off the external cortex of the calvarium by sharp dissection. Thirty milligrams of commercially prepared titanium particles was placed directly onto the surface of the bone, and the incision was closed. Mice were killed on day 10 thereafter, and each calvarium was excised, fixed, and decalcified in EDTA. After dehydration and paraffin embedding, serial sections measuring 5 μm in thickness were prepared from the 2-mm frontal bone to the intersection of sutures. For each animal, 3 sections of parietal bones obtained at 400-μm intervals were histochemically stained with hematoxylin and eosin and for tartrate-resistant acid phosphatase (TRAP) activity.

Immunohistochemistry. According to the manufacturer's instructions, OPN protein and TNFα were examined by immunohistochemistry with anti-mouse OPN antibody (product no. 18621; Immuno-Biological Laboratories) and anti-mouse TNFα antibody (product no. sc-1348; Santa Cruz Biotechnology), respectively. Briefly, sections were incubated overnight at 4°C with rabbit anti-mouse OPN antibody (1:20 dilution) and goat anti-mouse TNFα antibody (1:50 dilution). The sections then were incubated at room temperature for 30 minutes with biotinylated goat anti-rabbit IgG antibody and biotinylated rabbit anti-goat IgG antibody, respectively. Thereafter, sections were visualized with peroxidase-conjugated avidin and diaminobenzidine using a Vectastain kit (Vector).

Bone histomorphometry. Histomorphometric measurements were performed with a system consisting of a PC and image analysis software (Image Pro Plus 4.1; Media Cybernetics). Since the sagittal suture is irregular in shape in this model, we excluded from the measurement the area within 400 μm lateral to the sagittal suture so that an accurate assessment of bone resorption area could be obtained. The bone resorption area was measured as the eroded surface (ES) along the superior calvarial surface. The osteoclast surface (OcS) and osteoclast number (OcN) were determined in TRAP-stained sections. Osteoclasts were morphologically identified as large multinucleated cells located on the bone perimeter within resorption lacunae.

In vitro activation of bone marrow–derived macrophages (BMMs). Bone marrow stromal cells were obtained from the femoral bone marrow of OPN-deficient and WT mice. Cells were cultured at a density of 1×10^6/well in 24-well plates for 5 days in α-minimum essential medium (α-MEM)/10% fetal calf serum containing 50 ng/ml of macrophage colony-stimulating factor (M-CSF). To confirm the differentiation of stromal cells into macrophages, cultured cells from WT and OPN-deficient mice were diluted with the same solution and analyzed by fluorescence-activated cell sorting (FACS) for CD11b expression.

BMM cytokine secretion assay. BMMs were isolated from WT and OPN-deficient mice (2 mice for each genotype). BMMs of each genotype were divided into 3 groups, cultured for 12 hours with titanium particles, and the concentrations of TNFα and OPN in the media were measured with ELISA kits according to the manufacturer's protocols (Amersham Biosciences, BioSource International, and Immuno-Biological Laboratories, respectively). Multiplex suspension bead array immunoassays were performed using a Luminex 100 analyzer to identify cytokine protein expression in culture supernatants. A Mouse Cytokine 7-Plex kit (BioSource International) was used to specifically evaluate patterns of IL-1α, IL-1β, IL-6, IL-17, MCP-1, MIP-1α, and RANTES expression according to the user's manual.

BMM phagocytic assay. BMMs obtained from the marrow of the long bones of OPN-deficient and WT mice were cultured for 3 days at a density of 1×10^6 cells in 10-cm dishes and then exposed to fluorescence latex beads (Toray) for 1 hour at 37°C. The percentage of phagocytic macrophages was then analyzed by flow cytometry.

Western blot analysis of IκB degradation. Nucleated bone marrow cells were seeded on 35-mm–diameter dishes at a concentration of 5×10^6/dish. Cells were maintained for 3 days in α-MEM supplemented with 10% fetal calf serum, 100 units/ml of penicillin G, 100 μg/ml of streptomycin sulfate, 250 ng/ml of amphotericin B, and 50 ng/ml of M-CSF. On the third day, cells were exposed to titanium particles for various time periods ranging from 0 to 120 minutes. Cells were solubilized with Cell Lysis Buffer (Cell Signaling Technologies) supplemented with 1 m*M* phenylmethylsulfonyl fluoride and a protease inhibitor cocktail (Complete Mini; Roche Applied Science). Cell lysates (10 μg) were separated in sodium dodecyl sulfate–Tris glycine–polyacrylamide gels (4–20% gradient gel; Invitrogen) and blotted on to polyvinylidene difluoride membranes (Bio-Rad). The membranes were stained with anti-mouse IκBα polyclonal antibody (BioVision Research Products), and signals were visualized with a Vectastain Elite ABC kit (Vector). Membranes were reblotted with anti-mouse β-actin antibody (Santa Cruz Biotechnology) as a sample loading control.

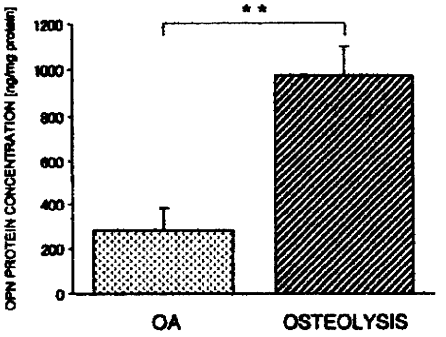

Figure 1. Osteopontin (OPN) protein levels in human periprosthetic osteolysis tissues. OPN protein levels were increased in interface membranes and capsules from aseptically loosened total hip implants (osteolysis) as compared with osteoarthritis (OA) synovium. Values are the mean and SEM. ** = $P < 0.001$.

Statistical analysis. Data are expressed as the mean ± SEM. Statistical evaluation was performed with the Mann-Whitney U test. P values less than 0.05 were considered significant.

RESULTS

Enhanced expression of OPN protein in human periprosthetic osteolysis tissues. We compared OPN protein expression levels in the interface membranes and capsules from patients with aseptically loosened total hip implants with the OPN protein expression in OA synovium (Figure 1). The findings of ELISA indicated that OPN protein was strongly increased in the periprosthetic osteolysis tissues.

Protection of OPN-deficient mice from particle-induced osteolysis. To investigate the function of OPN in particle-induced osteolysis, we used a previously established in vivo mouse calvaria resorption model that closely resembles aseptic loosening in humans (22). The calvariae of WT mice exposed to titanium particles generated a supracranial inflammatory response consisting of a fibrous membrane associated with abundant mononuclear cells (Figure 2A), which were identified by their morphometric appearance as being macrophages, foreign-body giant cells, fibroblasts, and osteoclasts. Importantly, these membranes contained numerous juxtacortical osteoclasts (Figures 2A, C, and E). Whereas the calvariae of OPN-deficient mice exposed to titanium particles generated an inflammatory membrane similar to that seen in WT animals (Figure 2B), the titanium

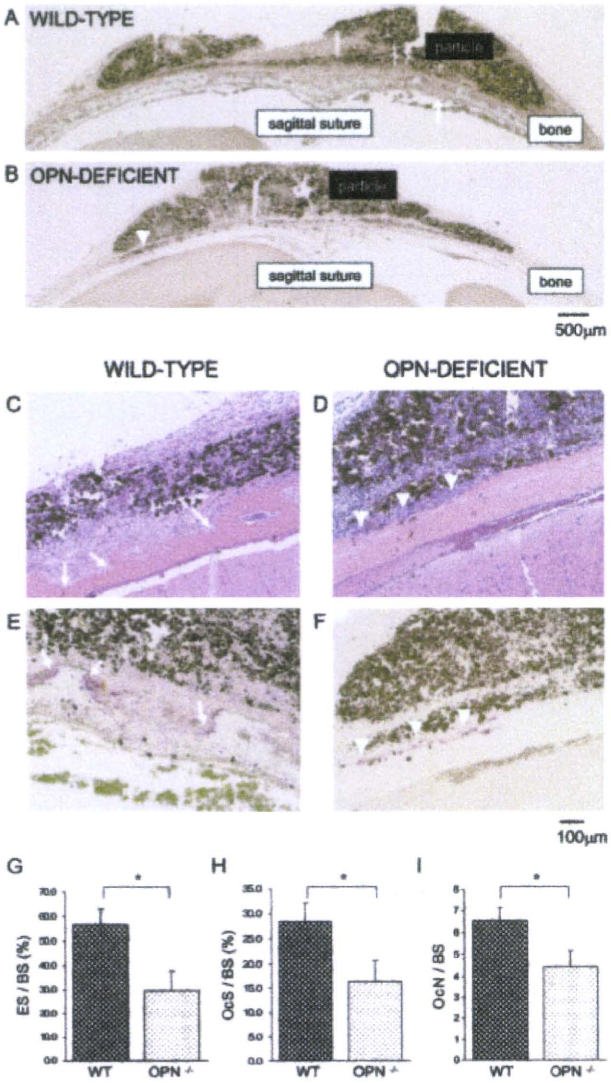

Figure 2. Protection of osteopontin (OPN)–deficient mice from particle-induced osteolysis in an in vivo calvaria resorption model. Sections of calvaria from wild-type (WT) or OPN$^{-/-}$ mice were stained with hematoxylin and eosin (**C** and **D**) and for tartrate-resistant acid phosphatase activity (**A**, **B**, **E**, and **F**). **A** and **B**, Sections of whole calvaria from a WT mouse and an OPN$^{-/-}$ mouse. **C–F**, Higher-magnification views of calvarial sections from WT and OPN$^{-/-}$ mice. Inflammatory reactions consisting of a fibrous membrane and osteoclastic bone resorption were widespread in WT mice (**arrows** in **A**, **C**, and **E**). These reactions were less severe in OPN$^{-/-}$ mice (**arrowheads** in **B**, **D**, and **F**). **G–I**, Quantification of particle-induced osteolysis and osteoclastogenesis. The eroded surface/bone surface (ES/BS) (**G**) measure indicates the bone resorption area on the superior calvarial surface >400 μm away from the sagittal suture. The osteoclast surface/bone surface (OcS/BS) (**H**) and osteoclast number/bone surface (OcN/BS) (**I**) measures were also determined outside of the suture area. Values are the mean and SEM. $* = P < 0.05$.

particle–induced bone resorption was attenuated in these animals (Figures 2B, D, and F). No enhancement of bone resorption activity was observed regardless of the genotypes in sham-operated mice (results not shown).

TRAP staining revealed the presence of osteoclasts in each resorption pit (Figures 2A, B, E, and F). However, the bone resorption area (representing the ES/bone surface [BS]) on the cortex was significantly reduced in osteolysis-induced OPN-deficient mice as compared with their WT littermates (Figure 2G). The OcS/BS and the OcN/BS were also significantly reduced in OPN-deficient mice as compared with their WT littermates (Figures 2H and I). Thus, osteoclastogenesis was impaired by OPN deficiency in this model.

Bone resorption lacunae were observed even in OPN-deficient osteoclasts. However, each bone resorption pit on the surface of OPN-deficient calvaria was shallow (Figures 2F and 3B), whereas penetration of the calvaria cortex was observed in WT animals as a result of active bone resorption (Figures 2E and 3A). The depth and area of each bone resorption pit were significantly reduced by OPN deficiency (Figures 3C and D). These data indicated that the function of each osteoclast was attenuated by OPN deficiency.

Enhanced expression of OPN protein and TNFα in mice with particle-induced osteolysis. Immunohistologic examination revealed that OPN protein was highly

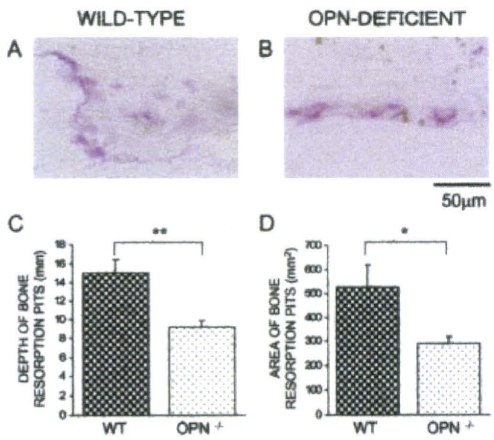

Figure 3. Smaller bone resorption pits in osteoclasts from osteopontin (OPN)–deficient mice. **A** and **B**, Morphologic features of osteoclasts from wild-type (WT) and OPN$^{-/-}$ mice. **C** and **D**, Quantification of the depth (**C**) and area (**D**) of bone resorption pits. Bone resorption pits were measured in high-power micrographs of tartrate-resistant acid phosphatase–stained sections. Values are the mean and SEM. $** = P < 0.001$; $* = P < 0.05$.

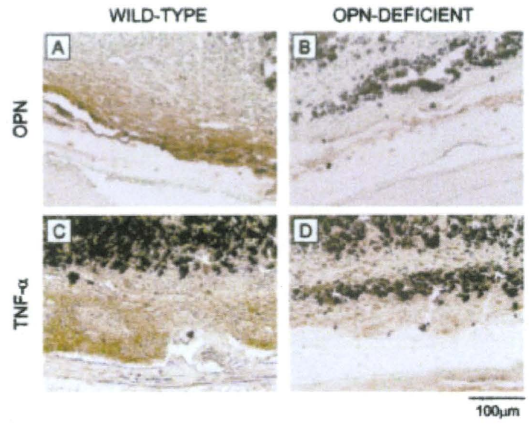

Figure 4. Expression of osteopontin (OPN) and tumor necrosis factor α (TNFα) in a murine calvaria resorption model. OPN protein expression in the membrane and bone surface of the bone resorption area was enhanced in wild-type (WT) animals (**A**) but was not detected in OPN$^{-/-}$ animals (**B**). TNFα expression in the membrane and bone surface of the bone resorption area was enhanced in WT animals (**C**), whereas it was hardly detected in OPN$^{-/-}$ animals (**D**). Color figure can be viewed in the online issue, which is available at http://www.arthritisrheum.org.

expressed in the membranous tissue and on the bone surface in the bone resorption area in WT mice (Figure 4A). No specific staining was seen in the membranous tissue or bone surface in OPN-deficient mice (Figure 4B), confirming the lack of OPN expression in these animals. TNFα, the inflammatory cytokine implicated in particle-induced osteolysis, was highly expressed in membranous tissue and on the bone surface in bone resorption areas in WT mice (Figure 4C), whereas TNFα expression was reduced in OPN-deficient mice (Figure 4D). These observations suggest that OPN may play a role in cytokine secretion from macrophages stimulated by wear particles.

Effect of OPN deficiency on cytokine secretion by BMMs in response to titanium particle treatment. To further investigate the effect of OPN deficiency in macrophages stimulated by particles, the secretion of TNFα and other osteolysis-associated cytokines was evaluated using cultured BMMs. FACS analysis indicated that ~70% of bone marrow stromal cells were differentiated into macrophages, and the number of CD11b-positive cells was similar in both genotypes (results not shown). The OPN concentration in the cell culture supernatants of BMMs from WT mice was significantly higher following exposure to titanium particles (Figure 5G). OPN was not detected in cell culture supernatants of OPN-deficient BMMs regardless of exposure to particles (data not shown).

TNFα levels were significantly lower in cell culture supernatants of BMMs from OPN-deficient mice as compared with BMMs from WT mice after exposure to titanium particles (Figure 5A). Furthermore, levels of the proinflammatory cytokines IL-1α, IL-1β, and IL-6 and the chemotactic factors MCP-1 and MIP-1α were significantly reduced in culture supernatants of BMMs from OPN-deficient mice (Figures 5B–F). In contrast, the secretion of IL-17 and RANTES was not affected by OPN deficiency (data not shown). These data indicate that OPN participates in particle-mediated osteoclastogenesis via orchestration of inflammatory cytokine secretion from BMMs.

Lack of effect of OPN deficiency on phagocytic activity of BMMs. To investigate the effect of OPN deficiency on BMM phagocytic activity, we analyzed latex bead phagocytosis in BMMs from WT and OPN-deficient mice. Flow cytometric analysis revealed that BMMs from OPN-deficient mice have a phagocytic capacity similar to that of BMMs from WT mice (Figures 6A–D). These results indicate that OPN does not act in the regulation of BMM phagocytosis, at least not in vitro.

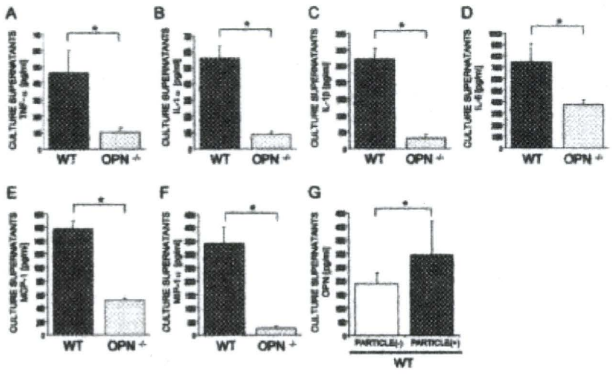

Figure 5. Osteolysis-associated cytokine concentrations in culture supernatants after exposure to titanium particles. Bone marrow–derived macrophages (BMMs) obtained from wild-type (WT) or osteopontin-deficient (OPN$^{-/-}$) mice were cultured with titanium particles for 12 hours. Concentrations of tumor necrosis factor α (TNFα) (**A**), interleukin-1α (IL-1α) (**B**), IL-1β (**C**), IL-6 (**D**), monocyte chemoattractant protein 1 (MCP-1) (**E**), and macrophage inflammatory protein 1α (MIP-1α) (**F**) in culture supernatants were determined. In addition, BMMs obtained from WT animals were cultured for 12 hours with or without titanium particles, and the OPN concentration in the culture supernatants was measured (**G**). Values are the mean and SEM. * = $P < 0.05$.

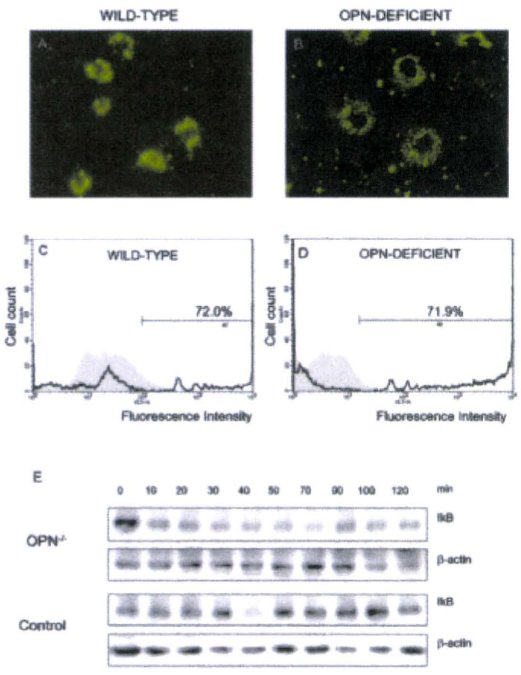

Figure 6. Phagocytic activity of bone marrow–derived macrophages (BMMs). **A** and **B,** BMMs obtained from the marrow of the long bones of wild-type (WT) and osteopontin-deficient ($OPN^{-/-}$) mice were exposed to fluorescence latex beads and incubated for 1 hour at 37°C (magnification × 400). **C** and **D,** The percentage of phagocytic macrophages in WT and $OPN^{-/-}$ mice was analyzed by flow cytometry. **E,** Impairment of phagocytosis-mediated IκB degradation in BMMs derived from $OPN^{-/-}$ mice. BMMs were isolated from 6-month-old $OPN^{-/-}$ mice and their WT control littermates. Cells were exposed to titanium particles for the indicated times. Transient IκB degradation, which causes NF-κB activation, was observed at 40 minutes after exposure in cells from control mice, while no obvious surge of IκB degradation was observed for up to 120 minutes in cells from $OPN^{-/-}$ mice. β-actin was used as a loading control. Color figure can be viewed in the online issue, which is available at http://www.arthritisrheum.org.

Phagocytosis-mediated IκB degradation in BMMs. To address the role of OPN on phagocytosis-mediated cytokine secretion, NF-κB activation was investigated in BMMs stimulated by titanium particles. BMMs from WT and OPN-deficient mice were exposed to titanium particles for various time periods (Figure 6E). Transient IκB degradation, which causes NF-κB activation, was clearly observed at 40 minutes after exposure in cells from control mice, while no obvious surge of IκB degradation was observed for up to 120 minutes in cells from OPN-deficient mice. Thus, phagocytosis-mediated NF-κB activation was impaired in BMMs from OPN-deficient mice.

DISCUSSION

The major cause of failure of long-term implants in patients with total joint replacements is aseptic loosening due to particle-induced osteolysis. A foreign-body, granulomatous response to material byproducts creates a chronic inflammatory reaction composed primarily of activated macrophages and fibroblasts. The periprosthetic tissues may produce high levels of proinflammatory cytokines (TNFα, IL-1, and IL-6, etc.), chemokines for macrophages, polymorphonuclear leukocytes and lymphocytes, prostanoids, and nitric oxide and superoxide metabolites (23,24). In the present study, we demonstrated that OPN is required for the progression of titanium particle–induced osteolysis in a murine calvaria model.

OPN protein and mRNA are expressed in macrophages in the periprosthetic tissue of patients with aseptically loosened prostheses (17). Here, we confirmed by ELISA elevated levels of OPN protein in the periprosthetic tissue. OPN is also expressed in human and murine granulomatous responses of diverse causes (15,16) and is required for functional granuloma formation (24). It is notable that OPN production is induced by a number of mediators that are abundantly expressed during cell-mediated/granulomatous inflammation (25). In particular, staining of TNFα was diminished in OPN-deficient animals, implicating OPN in the regulation of TNFα secretion in particle-induced osteolysis. TNFα, a potent cytokine produced by monocytes in response to titanium, is known to activate osteoclasts to resorb bone, and it has been shown to be critically involved in wear debris–induced osteolysis in vivo (5,22,26). TNFα also prompts osteoclastogenesis in cultured murine bone marrow (26). In this study, in vitro experiments with BMMs exposed to titanium particles indicated that OPN was indispensable for TNFα secretion by macrophages.

Decreased depth of bone resorption pits in OPN-deficient mice with particle-induced osteolysis suggested that OPN was indispensable for osteoclast function, as has been reported elsewhere (Figure 3). Osteoclasts express OPN, which stimulates bone resorption and osteoclast motility, thus increasing the number and depth of resorption pits (27). Osteoclasts from OPN-deficient mice are hypomotile and less active in bone resorption than are osteoclasts from WT mice. Thus, the function of secreted OPN as an osteoclast autocrine factor may be to stimulate cell motility and adhesion related to bone resorption. Since osteoclasts are actively migrating cells, hypomotility decreases bone resorption (27). Adhesion, organization for migration, and organi-

zation for resorption are sequential events that are necessary for osteoclast function (28), and OPN stimulates each of these events. Furthermore, an intracellular form of OPN that activates macrophages and metastatic cells through association with the CD44 complex (29) functions in the formation and activity of osteoclasts (30).

Phagocytic uptake involves actin dynamics, including polymerization, bundling, contraction, severing, and depolymerization of actin filaments. The Rho GTP binding proteins are signaling elements critical to the control of actin reorganization during a variety of phagocytic signaling processes (31,32). Osteoclasts stimulated with OPN were shown to recapitulate the effects of Rho and Cdc42 in phosphatidylinositol 4,5-bisphosphate association with Wiscott-Aldrich syndrome protein as well as actin ring formation (31,33,34). Thus, we speculated that OPN deficiency might affect the phagocytic activity of BMMs. However, the findings of our in vitro studies excluded this possibility (Figure 6) and indicated that the regulation of proinflammatory cytokines by OPN is independent of phagocytotic activity.

Our in vitro studies with BMMs from WT mice revealed increased OPN concentrations in culture supernatants after exposure to titanium particles. This result may be associated with the observation that OPN mRNA and protein expression from macrophages are enhanced by TNFα stimulation (35,36). Moreover, we confirmed that OPN protein expression levels were enhanced in human periprosthetic osteolysis tissues as compared with OA synovium. We speculate that the cytokine milieu produced by macrophages in particle-exposed synovium induces the overproduction of OPN. Our results also showed that levels of TNFα and other inflammatory cytokines (IL-1α, IL-1β, IL-6, MCP-1, and MIP-1α) were reduced in culture supernatants of cells from OPN-deficient mice via NF-κB inactivation, implicating OPN in the secretion of a variety of inflammatory cytokines by macrophages.

OPN activates the NF-κB transcription factor pathway, which is known to play a critical role in the production of many inflammatory cytokines and chemokines (37). NF-κB is the main factor involved in the transcription of MCP-1 and MIP-1α (38,39). Thus, inflammatory cytokine secretion is enhanced by OPN through NF-κB–mediated pathways. Overproduction of OPN, in turn, amplifies inflammation through proinflammatory chemokines and cytokines and promotes the migration and recruitment of inflammatory cells into the inflamed synovium (37). This mechanism, which is mediated by OPN, is likely to play a key role in periprosthetic osteolysis. Taken together, OPN and inflammatory cytokines may constitute a positive feedback loop in the periprosthetic soft tissues and may promote chronic inflammation.

We used titanium particles in this study. In the clinical setting, the most widely accepted implant configuration includes a metal component articulating against a polyethylene component (40). Today, total joint replacement with metal on ultrahigh molecular weight polyethylene is the international standard of care for degenerative joint disorders (40,41). Although it seems that polyethylene particles are the most common inducer of osteolysis around joint replacement implants (42), titanium particles have been commonly used for murine calvaria bone resorption models (5,22,40,42–44). Taki et al (44) recently reported that similar mechanisms were responsible for osteolysis induced by polyethylene and titanium particles.

Some current studies focused on the role of adherent endotoxin on titanium particles and particle-induced osteolysis (44–47). As reported by Ragab et al (45), it is unavoidable that substantial amounts of endotoxin adhere to the commercially available titanium particles even if the particles are sterilized. In addition, orthopedic implant surfaces contain significant levels of adherent endotoxin (45). Although the clinical relevance of adherent endotoxin in aseptic loosening is a subject of controversy, it increases the biologic effects of orthopedic wear particles in cell culture as well as in vivo (47). Tatro et al (46) demonstrated that systemically derived endotoxin accumulates when "endotoxin-free," commercially pure titanium particles are implanted on murine calvaria. This does not suggest that the wear particles are unimportant, but that they act together with endotoxin to induce osteolysis (46). Taken together, the balance between accumulation and clearance of endotoxin may regulate the rate of osteolysis in the murine calvaria model as well as in patients with aseptic loosening of a prosthesis (46).

Our findings provide evidence that in the absence of OPN, wear debris–induced osteolysis was impaired. From this standpoint, periprosthetic osteolysis might be blocked by reducing the function of OPN. Although we did not examine them in this study, OPN inhibitors, such as $\alpha v\beta 3$ antagonist and antibody against OPN, are promising agents for protecting against periprosthetic osteolysis. The use of TNFα antagonists to treat inflammatory diseases such as RA has dramatically increased in recent years, and a recent study demonstrated the effectiveness of TNFα inhibitors in the treatment of

aseptic loosening and wear debris–induced osteolysis (5). However, the enormous cost of this type of treatment restricts the use of such biologic drugs to a small number of selected patients with severe disease (19). Development of nonpeptide antagonists against OPN activity could solve such problems (19).

In conclusion, we have shown that OPN plays critical roles in wear debris–induced osteolysis. Our data suggest that OPN is a candidate for a therapeutic target in periprosthetic osteolysis.

ACKNOWLEDGMENTS

The authors would like to kindly thank Dr. Akimoto Nimura for assistance with the FACS analysis and Miyoko Ojima for expert help with the histologic analysis.

AUTHOR CONTRIBUTIONS

All authors were involved in drafting the article or revising it critically for important intellectual content, and all authors approved the final version to be published. Dr. Asou had full access to all of the data in the study and takes responsibility for the integrity of the data and the accuracy of the data analysis.

Study conception and design. Rittling, Okawa, Shinomiya, Muneta, Denhardt, Noda, Asou.

Acquisition of data. Shimizu, Okuda, Kato, Tsuji, Asou.

Analysis and interpretation of data. Shimizu, Okuda, Tsuji, Asou.

REFERENCES

1. Harris WH. Wear and periprosthetic osteolysis: the problem. Clin Orthop Relat Res 2001;393:66–70.
2. Jacobs JJ, Roebuck KA, Archibeck M, Hallab NJ, Glant TT. Osteolysis: basic science. Clin Orthop Relat Res 2001;393:71–7.
3. Willert HG. Reactions of the articular capsule to wear products of artificial joint prostheses. J Biomed Mater Res 1977;11:157–64.
4. Green TR, Fisher J, Stone M, Wroblewski BM, Ingham E. Polyethylene particles of a 'critical size' are necessary for the induction of cytokines by macrophages in vitro. Biomaterials 1998;19:2297–302.
5. Childs LM, Goater JJ, O'Keefe RJ, Schwarz EM. Effect of anti-tumor necrosis factor-α gene therapy on wear debris-induced osteolysis. J Bone Joint Surg Am 2001;83-A:1789–97.
6. Nakashima Y, Sun DH, Trindade MC, Chun LE, Song Y, Goodman SB, et al. Induction of macrophage C-C chemokine expression by titanium alloy and bone cement particles. J Bone Joint Surg Br 1999;81:155–62.
7. Shanbhag AS, Hasselman CT, Rubash HE. Inhibition of wear debris mediated osteolysis in a canine total hip arthroplasty model. Clin Orthop Relat Res 1997;344:33–43.
8. Granchi D, Verri E, Ciapetti G, Stea S, Savarino L, Sudanese A, et al. Bone-resorbing cytokines in serum of patients with aseptic loosening of hip prostheses. J Bone Joint Surg Br 1998;80:912–7.
9. Teitelbaum SL. Bone resorption by osteoclasts. Science 2000;289:1504–8.
10. Childs LM, Paschalis EP, Xing L, Dougall WC, Anderson D, Boskey AL, et al. In vivo RANK signaling blockade using the receptor activator of NF-κB:Fc effectively prevents and ameliorates wear debris-induced osteolysis via osteoclast depletion without inhibiting osteogenesis. J Bone Miner Res 2002;17:192–9.
11. Granchi D, Amato I, Battistelli L, Ciapetti G, Pagani S, Avnet S, et al. Molecular basis of osteoclastogenesis induced by osteoblasts exposed to wear particles. Biomaterials 2005;26:2371–9.
12. Denhardt DT, Noda M. Osteopontin expression and function: role in bone remodeling. J Cell Biochem Suppl 1998;30/31:92–102.
13. Denhardt DT, Noda M, O'Regan AW, Pavlin D, Berman JS. Osteopontin as a means to cope with environmental insults: regulation of inflammation, tissue remodeling, and cell survival. J Clin Invest 2001;107:1055–61.
14. Asou Y, Rittling SR, Yoshitake H, Tsuji K, Shinomiya K, Nifuji A, et al. Osteopontin facilitates angiogenesis, accumulation of osteoclasts, and resorption in ectopic bone. Endocrinology 2001;142:1325–32.
15. Saeki Y, Mima T, Ishii T, Ogata A, Kobayashi H, Ohshima S, et al. Enhanced production of osteopontin in multiple myeloma: clinical and pathogenic implications. Br J Haematol 2003;123:263–70.
16. Standal T, Hjorth-Hansen H, Rasmussen T, Dahl IM, Lenhoff S, Brenne AT, et al. Osteopontin is an adhesive factor for myeloma cells and is found in increased levels in plasma from patients with multiple myeloma. Haematologica 2004;89:174–82.
17. Zreiqat H, Kumar RK, Markovic B, Zicat B, Howlett CR. Macrophages at the skeletal tissue-device interface of loosened prosthetic devices express bone-related genes and their products. J Biomed Mater Res A 2003;65:109–17.
18. Yoshitake H, Rittling SR, Denhardt DT, Noda M. Osteopontin-deficient mice are resistant to ovariectomy-induced bone resorption. Proc Natl Acad Sci U S A 1999;96:8156–60.
19. Yumoto K, Ishijima M, Rittling SR, Tsuji K, Tsuchiya Y, Kon S, et al. Osteopontin deficiency protects joints against destruction in anti-type II collagen antibody-induced arthritis in mice. Proc Natl Acad Sci U S A 2002;99:4556–61.
20. Rittling SR, Denhardt DT. Osteopontin function in pathology: lessons from osteopontin-deficient mice. Exp Nephrol 1999;7:103–13.
21. Rittling SR, Matsumoto HN, McKee MD, Nanci A, An XR, Novick KE, et al. Mice lacking osteopontin show normal development and bone structure but display altered osteoclast formation in vitro. J Bone Miner Res 1998;13:1101–11.
22. Schwarz EM, Benz EB, Lu AP, Goater JJ, Mollano AV, Rosier RN, et al. Quantitative small-animal surrogate to evaluate drug efficacy in preventing wear debris-induced osteolysis. J Orthop Res 2000;18:849–55.
23. Goodman SB, Huie P, Song Y, Schurman D, Maloney W, Woolson S, et al. Cellular profile and cytokine production at prosthetic interfaces: study of tissues retrieved from revised hip and knee replacements. J Bone Joint Surg Br 1998;80:531–9.
24. Goodman SB, Trindade M, Ma T, Genovese M, Smith RL. Pharmacologic modulation of periprosthetic osteolysis. Clin Orthop Relat Res 2005;430:39–45.
25. O'Regan A, Berman JS. Osteopontin: a key cytokine in cell-mediated and granulomatous inflammation. Int J Exp Pathol 2000;81:373–90.
26. Merkel KD, Erdmann JM, McHugh KP, Abu-Amer Y, Ross FP, Teitelbaum SL. Tumor necrosis factor-α mediates orthopedic implant osteolysis. Am J Pathol 1999;154:203–10.
27. Chellaiah MA, Soga N, Swanson S, McAllister S, Alvarez U, Wang D, et al. Rho-A is critical for osteoclast podosome organization, motility, and bone resorption. J Biol Chem 2000;275:11993–2002.
28. Kanehisa J, Heersche JN. Osteoclastic bone resorption: in vitro analysis of the rate of resorption and migration of individual osteoclasts. Bone 1988;9:73–9.
29. Zohar R, Suzuki N, Suzuki K, Arora P, Glogauer M, McCulloch CA, et al. Intracellular osteopontin is an integral component of the CD44-ERM complex involved in cell migration. J Cell Physiol 2000;184:118–30.
30. Suzuki K, Zhu B, Rittling SR, Denhardt DT, Goldberg HA, McCulloch CA, et al. Colocalization of intracellular osteopontin

with CD44 is associated with migration, cell fusion, and resorption in osteoclasts. J Bone Miner Res 2002;17:1486–97.
31. Caron E, Hall A. Identification of two distinct mechanisms of phagocytosis controlled by different Rho GTPases. Science 1998; 282:1717–21.
32. Chellaiah MA. Regulation of actin ring formation by rho GTPases in osteoclasts. J Biol Chem 2005;280:32930–43.
33. Blanchoin L, Amann KJ, Higgs HN, Marchand JB, Kaiser DA, Pollard TD. Direct observation of dendritic actin filament networks nucleated by Arp2/3 complex and WASP/Scar proteins. Nature 2000;404:1007–11.
34. Cox D, Chang P, Zhang Q, Reddy PG, Bokoch GM, Greenberg S. Requirements for both Rac1 and Cdc42 in membrane ruffling and phagocytosis in leukocytes. J Exp Med 1997;186:1487–94.
35. Denhardt DT, Guo X. Osteopontin: a protein with diverse functions. FASEB J 1993;7:1475–82.
36. Patarca R, Saavedra RA, Cantor H. Molecular and cellular basis of genetic resistance to bacterial infection: the role of the early T-lymphocyte activation-1/osteopontin gene. Crit Rev Immunol 1993;13:225–46.
37. Xu G, Nie H, Li N, Zheng W, Zhang D, Feng G, et al. Role of osteopontin in amplification and perpetuation of rheumatoid synovitis. J Clin Invest 2005;115:1060–7.
38. Ueda A, Okuda K, Ohno S, Shirai A, Igarashi T, Matsunaga K, et al. NF-κB and Sp1 regulate transcription of the human monocyte chemoattractant protein-1 gene. J Immunol 1994;153:2052–63.
39. Grove M, Plumb M. C/EBP, NF-κB, and c-Ets family members and transcriptional regulation of the cell-specific and inducible macrophage inflammatory protein 1α immediate-early gene. Mol Cell Biol 1993;13:5276–89.
40. Von Knoch M, Jewison DE, Sibonga JD, Sprecher C, Morrey BF, Loer F, et al. The effectiveness of polyethylene versus titanium particles in inducing osteolysis in vivo. J Orthop Res 2004;22:237–43.
41. Kurtz SM, Muratoglu OK, Evans M, Edidin AA. Advances in the processing, sterilization, and crosslinking of ultra-high molecular weight polyethylene for total joint arthroplasty. Biomaterials 1999; 20:1659–88.
42. Ulrich-Vinther M, Carmody EE, Goater JJ, K Soballe, O'Keefe RJ, Schwarz EM. Recombinant adeno-associated virus-mediated osteoprotegerin gene therapy inhibits wear debris-induced osteolysis. J Bone Joint Surg Am 2002;84-A:1405–12.
43. Soloviev A, Schwarz EM, Darowish M, O'Keefe RJ. Sphingomyelinase mediates macrophage activation by titanium particles independent of phagocytosis: a role for free radicals, NFκB, and TNFα. J Orthop Res 2005;23:1258–65.
44. Taki N, Tatro JM, Nalepka JL, Togawa D, Goldberg VM, Rimnac CM, et al. Polyethylene and titanium particles induce osteolysis by similar, lymphocyte-independent, mechanisms. J Orthop Res 2005;23:376–83.
45. Ragab AA, Van De Motter R, Lavish SA, Goldberg VM, Ninomiya JT, Carlin CR, et al. Measurement and removal of adherent endotoxin from titanium particles and implant surfaces. J Orthop Res 1999;17:803–9.
46. Tatro JM, Taki N, Islam AS, Goldberg VM, Rimnac CM, Doerschuk CM, et al. The balance between endotoxin accumulation and clearance during particle-induced osteolysis in murine calvaria. J Orthop Res 2007;25:361–9.
47. Taki N, Tatro JM, Lowe R, Goldberg VM, Greenfield EM. Comparison of the roles of IL-1, IL-6, and TNFα in cell culture and murine models of aseptic loosening. Bone 2007;40:1276–83.

J Orthop Sci (2010) 15:161
DOI 10.1007/s00776-010-1461-5

JOURNAL OF
ORTHOPAEDIC SCIENCE

Editorial

Envisioning the evolution of orthopedic surgery in the twenty-first century

KENICHI SHINOMIYA

Department of Orthopaedic and Spinal Surgery, Graduate School of Medical and Dental Science, Tokyo Medical and Dental University, 1-5-45 Yushima, Bunkyo-ku, Tokyo 113-8519, Japan

Thanks to medical advances, Japanese society is aging at an astonishing rate; by the middle of the twenty-first century, the number of Japanese over the age of 100 will likely reach an unprecedented level. In light of this trend, our 83rd Annual Meeting, to be held May 27–30, 2010, has adopted the theme "A century for centenarians: how advances in orthopedics can help." Clearly, our common goal is not simply to live such a long life at all costs; unless we can enjoy happy and active lives, living beyond 100 years has little meaning.

In the latter half of the 1970s, when I was studying to become an orthopedic surgeon and spinal surgery specialist, the average life expectancy in Japan was approximately 10 years less than it is now. In the intervening years, our target diseases have changed dramatically: for example, lumbar spinal canal stenosis, first reported by Verviest in 1950, has become a common surgical disease, and minimally invasive decompression and fixation procedures are now widely performed. Moreover, in the field of cervical myelopathy, the idea of extensive simultaneous multisegment decompression was introduced by Kirita in 1968, leading to the various approaches to laminoplasty (Hirabayashi, Kurokawa, Itoh, Miyazaki) that are being applied to most cases of cervical spondylotic and OPLL myelopathy. Similarly, as reported by Yamaura in 1976, the anterior floating method of OPLL, which also employs simultaneous decompression, has become the procedure of choice in cases of severe compression of 60% or more of the spinal canal. Minimally invasive procedures have also come to play a central role in instrumentation surgery and in treatment of vertebral body fractures due to osteoporosis. Healthy bones and joints comprise the vital foundation that supports active centenarians, and it is clear that advances in spinal and joint surgery have contributed significantly to maintaining bone and joint health.

I entered the research field of spinal cord monitoring more than 30 years ago after being impressed by the research of Kurokawa and Tamaki. I have come to believe that my ability to have an eye for spinal cord monitoring during surgery has helped me to refine my spinal surgical techniques. As for the important issue of "disciplined training," despite my having had relatively limited exposure at a university hospital to spinal surgeries that could be considered "training," I was fortunate to have had an outstanding teacher who instilled the basics of spine surgery in me. That experience, as well as my exposure to many actual cases while on duty at related hospitals, gave me the confidence I required in my field. Evidently, finding an excellent mentor is the key to making progress as a surgeon.

In the next decade, the Japanese medical community will be focused on the issue of maintaining quality. Orthopedics covers a tremendously broad spectrum of bone and joint diseases, and in recent years the boundaries between the various fields of medicine have tended to become blurred as competition between these fields has heightened. In addition, we are approaching an era in which patients might cease to recognize our qualifications or expertise unless we can guarantee the level of expert treatment they demand. The basic requirements of a qualified physician are the abilities to make an appropriate diagnosis based on extensive knowledge, undertake appropriate treatment, and refer a patient to an appropriate treatment environment. Moreover, because of the great advances made by the medical community, patients now place greater expectations on physicians who specialize in advanced areas of medicine. Transparency about our knowledge and technical capabilities is likewise essential so that those outside our area of specialization can make informed decisions. Therefore, we need an efficient education and training system that imparts appropriate knowledge as well as the transparency to enable the general public to evaluate our techniques.

In conclusion, I believe that providing a team of outstanding teachers across Japan along with a harmonized training system for specialists will enable us to adapt to the evolution of orthopedic surgery in the twenty-first century. This combination of excellent mentors and an efficient educational and training system will do much to cultivate the next generation of specialists.

Offprint requests to: K. Shinomiya

The Roles of TNFR1 in Lipopolysaccharide-Induced Bone Loss: Dual Effects of TNFR1 on Bone Metabolism via Osteoclastogenesis and Osteoblast Survival

Hiroki Ochi,[1] Yasushi Hara,[1] Masahiro Tagawa,[1] Kenichi Shinomiya,[2] Yoshinari Asou[2]

[1]Division of Veterinary Surgery, Department of Veterinary Science, Faculty of Veterinary Medicine, Nippon Veterinary and Life Science University, 1-7-1 Kyonan-cho, Musashino, Tokyo, Japan, [2]Department of Orthopaedics Surgery, Tokyo Medical and Dental University, 1-5-45 yushima bunkyo-ku, Tokyo, 13-8519, Japan

Received 30 May 2009; accepted 10 September 2009
Published online 4 November 2009 in Wiley InterScience (www.interscience.wiley.com). DOI 10.1002/jor.21028

ABSTRACT: LPS (lipopolysaccharide), a major constituent of Gram-negative bacteria, regulates proliferation and differentiation of osteoclasts directly or indirectly. This study sought to investigate the functions of the RANK/RANKL pathway in LPS-induced bone loss in vivo. Wild-type mice or TNFR1−/− mice were injected LPS with or without osteoprotegerin (OPG) and analyzed histologically. Bone volume was reduced by LPS injection in all groups, and OPG administration prevented the LPS-induced bone loss regardless of genotypes. LPS-induced enhancement of osteoclastogenesis in wild-type mice was blocked by OPG administration. LPS or OPG did not affect osteoclastogenesis in TNFR1−/− mice. Interestingly, osteoblast surface was remarkably reduced in LPS-treated TNFR1−/− mice as a result of enhanced osteoblast apoptosis. TRAIL, induced by TNF-α in BMC, triggered apoptosis of primary osteoblast only when TNFR1 signal was ablated in vitro. In conclusion, RANK signaling plays a prominent role in osteoclastogenesis downstream of LPS. Furthermore, TNFR1 regulates bone metabolism through not only the regulation of osteoclast differentiation but also osteoblast survival. © 2009 Orthopaedic Research Society. Published by Wiley Periodicals, Inc. J Orthop Res 28:657–663, 2010

Keywords: lipopolysaccharide; osteoprotegerin; TNFR1; osteoclast; osteoblast

Bacterial infections are associated with rapid bone destruction in osteomyelitis, bacterial arthritis, and infected orthopedic implant failure.[1,2] Lipopolysaccharide (LPS), a major constituent of Gram-negative bacteria, is one of the molecular factors plays a major role in bone resorption in periodontitis or ostemyelitis [1] by stimulating the the production of proinflammatory cytokines.[3,4] LPS stimulates synthesis of tumor necrosis factor-α (TNF-α), via NF-κB activation.[5,6] At the cellular level, TNF-α affects bone structure through the inhibition of osteoblast function and stimulation of osteoclast formation both directly and indirectly.[7–9] TNF-α directly targets osteoclasts and their precursors, and that deletion of its type-1 receptor (TNFR1) lessens osteoclastogenesis and impacts RANK signaling molecules.[9,10] LPS injection induces osteoclastogenesis via TNF-α ligation of TNFR1 in vivo.[10,11] Therefore, TNF-α can be considered to be a critical link between chronic inflammation and bone loss. Receptor activator of NF-κB ligand (RANKL) was identified as an essential factor in osteoclastogenesis.[12,13] Osteoblasts/stromal cells produce a soluble decoy receptor for RANKL, osteoprotegerin (OPG), which interrupts the interaction between RANKL and RANK to inhibit osteoclast formation both in vivo and in vitro.[12,14] LPS enhance RANKL production and suppress OPG production from osteoblasts in vitro.[15–17] Moreover, LPS can enhance the survival, fusion, and activation of osteoclasts independent of IL-1, TNF-α, and RANKL.[18] Thus, osteoclastogenesis is regulated by variety of signaling pathways downstream of LPS. However, it remains to be well understood which pathways are prominent in vivo. This study sought to investigate the relative importance of the direct effect of LPS, RANK/RANKL-mediated pathway and TNF-α/TNFR1-mediated pathway in LPS-induced bone loss in vivo.

Correspondence to: Yoshinari Asou (T: +81-3-5803-5279; F: +81-3-5803-5281; E-mail: aso.orth@tmd.ac.jp)

MATERIALS AND METHODS

Mice

Male wild-type or TNFR1−/− mice on the C57BL/6 background were obtained from Jackson Laboratory (Bar Harbor, ME, USA). All studies were approved by the institutional animal care committee.

Histological Analysis

Male mice (6–8 months, $n = 5–7$) were injected with 20 mg/kg body weight LPS (Sigma, St. Louis, MO, USA) or phosphate-buffered saline (PBS) subcutaneously on day 0. PBS or recombinant human OPG (Sankyo-Daiichi Co., Ltd., Tokyo, Japan) was given intraperitoneally on day 0 and day 1. All mice were sacrificed 48 h after LPS injection. Tibiae of each mouse were fixed in 4% paraformaldehyde for decalcified samples or in 70% ethanol for undecalcified samples. For decalcification, samples were treated with EDTA, dehydrated, and embedded in paraffin, then sectioned at a 6-μm thickness. Undecalcified samples were dehydrated, embedded in glycol metacrylate, sectioned, and stained for TRAP activity and ALP activity. Trabecular bone of the tibiae 200 to 600 μm away from growth plate was evaluated for histomorphometry using an image analyzer (Image pro plus, Planetron Inc., Tokyo, Japan). The abbreviations for histomorphometric parameters were according to the recommendation by the American Society of Bone and Mineral Research Histomorphometry Nomenclature Committee.[19]

Flow Cytometry Analysis

Bone marrow cells were isolated from the bone marrow by flushing with culture medium using a 21-gauge needle. Bone

marrow cells were incubated for 30 min with a FITC-conjugated monoclonal antimouse antibody against CD11b or Phycoerythrin-conjugated monoclonal antimouse antibody against TRAIL (eBioscience, San Diego, CA, USA). After washing in PBS, cells were diluted in 1 mL 1% paraformaldehyde and subjected to FACS analysis. Samples were analyzed using a FACScan flow cytometer (BD Biosciences, Franklin Lakes, NJ, USA).

Culture of Primary Mouse Osteoblastic Cells

Primary osteoblastic cells were isolated from 1-day-old mouse calvariae after five routine sequential digestions with 0.1% collagenase (Wako, Tokyo, Japan) and 0.2% dispase (Godo Shusei, Tokyo, Japan) as previously described.[20] Osteoblastic cells were combined and cultured at 37°C in α-MEM supplemented with 10% FCS under 5% CO_2 in air.

Terminal Deoxynucleotidyltransferase-Mediated UTP End Labeling (TUNEL) Assay

TUNEL assays were conducted using decalcified sections of femoral bones according to the manufacturer's instruction (TaKaRa, Tokyo, Japan). The number of TUNEL-positive cells was quantitated in the femoral bone marrow of paraffin-embedded samples.

Measurement of Cellular Injury

Primary osteoblasts (3×10^3 cells/dish), plated in 100 μL α-MEM supplemented with 10% FBS, were incubated at 37°C in 96-well dishes. After 2 days of culture, the medium was changed to 100 μL α-MEM supplemented with 10% FBS. Subsequently, cells were treated with TRAIL (Sigma) or Tween20, for positive control. After 24 h of culture, cellular injury was quantitated by the measurement of lactate dehydrogenase (LDH) release using an LDH-cytotoxicity assay kit (WAKO, Tokyo, Japan).

Measurement of Caspase Activity

Primary osteoblasts (3×10^6 cells/10-cm dish), plated in 100 μL α-MEM supplemented with 10% FBS, were incubated at 37°C. After 2 days of culture, the medium was changed to 100 μL α-MEM supplemented with 10% FBS. Subsequently, cells were treated with TRAIL for 6 hours (100 ng/mL, Sigma) or vehicle, for negative control. Caspase3 activity was quantified by caspase colorimetric assay kit (Clontech, Palo Alto, CA, USA). Representative set of results was selected from three independent experiments for display.

RESULTS

LPS-induced bone reduction was ameliorated by OPG administration. LPS stimulates bone resorption in vivo. To examine the effect of OPG on LPS-induced bone resorption, wild-type mice were injected with LPS in the presence or absence of OPG. Following sacrifice 48 h after injection, LPS treatment reduced BV/TV approximately 40% in the proximal region of tibial bones in wild-type mice (Fig. 1a). OPG administration reversed the LPS-induced bone loss in a dose-dependent manner. OPG administration at a dose of 0.5 mg/kg was sufficient to maintain bone volume within basal levels (Fig. 1a). As LPS treatment induces osteoclastogenesis through a TNFR1-dependent pathway,[10] TNFR1−/− mice were also injected with LPS in the presence or absence of OPG to investigate the roles of TNF-α and RANKL in LPS-induced osteoclastogenesis. TNF-α mRNA expression levels of bone marrow cells in wild-type and TNFR1−/− mice were similary enhanced 1 h after LPS injection (data not shown). Histomorphometric analysis, however, indicated that BV/TV was significantly reduced in LPS-injected TNFR1−/− mice (Fig. 1b). The reduction in bone volume was partially reversed by OPG treatment (Fig. 1b), but not significantly.

LPS Enhancement of Osteoclastogenesis Through TNFR1 and RANK Pathways

Histological analysis revealed Oc.S/BS and N.Oc/BS were increased in LPS-treated wild-type mice (Fig. 2b, g, and h). OPG treatment suppressed the observed LPS-induced osteoclastogenesis in a dose-dependent manner (Fig. 2g and h). Treatment with 0.5 mg/kg OPG completely reversed the changes in N.Oc/BS, returning these values to basal levels (Fig. 2g and h). In contrast, LPS and OPG had little effect on N.Oc/BS and Oc.S/BS

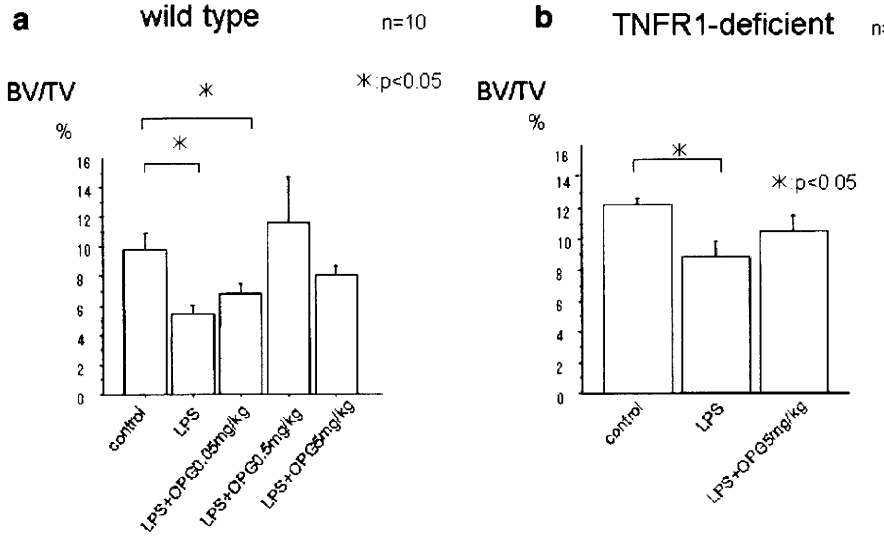

Figure 1. Histological analysis (a, b) indicated that the trabecular bone volume was significantly reduced in both wild-type (a) and TNFR1−/− (b) mice. Also, OPG administration inhibited the LPS-induced bone loss in wild-type animals in a dose-dependent manner (a), and bone volume was partially rescued by OPG injection in TNFR1−/− mice (b). Bars, ±SD. *$p < 0.05$ compared with control. Asterisk indicates statistically significant difference ($p < 0.05$).

in TNFR1−/− mice in comparison with wild-type mice (Fig. 2d–f, j, and k). Although urinary deoxypyridinoline, a marker for bone resorption, was increased the day after LPS injection in wild-type mice (Fig. 2i), these levels were unaffected by LPS or OPG treatment of TNFR1−/− mice (Fig. 2l). These results indicated TNFR1-mediated RANK/RANKL signaling plays a dominant role in LPS-induced osteoclastogenesis and osteoclastic bone resorption. To investigate the effect of TNFR1 and OPG on osteoclast precursors in the bone marrow, bone marrow cells were analyzed by flow cytometry. Two days after LPS injection (20 mg/kg), the numbers of CD11b-positive osteoclast precursors were increased in wild-type mice (Fig. 3a and b). In contrast, the population of CD11b-positive cells in the bone marrow of TNFR1−/− mice was not affected by LPS injection (Fig. 3d and e), indicating that TNFR1-mediated signaling is necessary for LPS-induced enhancement of the osteoclast precursor population in the bone marrow. OPG injection (5 mg/kg) did not affect the composition of the CD11b-positive cell population, regardless of genotype (Fig. 3c and f), indicating that RANK/RANKL signaling plays a role in osteoclast differentiation, rather than regulation of the osteoclast precursor population.

LPS Treatment-Induced High Turnover Osteopenia in Wild-Type Mice, but Low Turnover Levels in TNFR1-Deficient Mice

Next, we investigated the effect of LPS on bone formation. Forty-eight hours after LPS injection, the ALP-positive area and Ob.S/BS was increased as a result of high turnover osteopenia in wild-type mice (Figs. 2 and 4a). OPG treatment reduced these parameters to basal levels (Fig. 4a). In contrast, the ALP-positive area and Ob.S/BS were remarkably reduced in LPS-treated TNFR1−/− mice (Figs. 2 and 4c). Although serum osteocalcin levels were increased in wild-type mice immediately after LPS administration (Fig. 4b), the enhancement of osteocalcin levels was attenuated by in TNFR1−/− deficiency (Fig. 4d). Thus, TNFR1-mediated signaling was indispensable for the transient enhancement of bone formation during the acute phase of inflammation.

Susceptibility for TRAIL Was Induced by TNFR1-Deficiency in Murine Osteoblast

To address the mechanisms governing the reduction in osteoblasts in LPS-treated TNFR1−/− mice, we investigated the effect of LPS on osteoblast survival. TUNEL-positive cells were abundantly observed on the surface

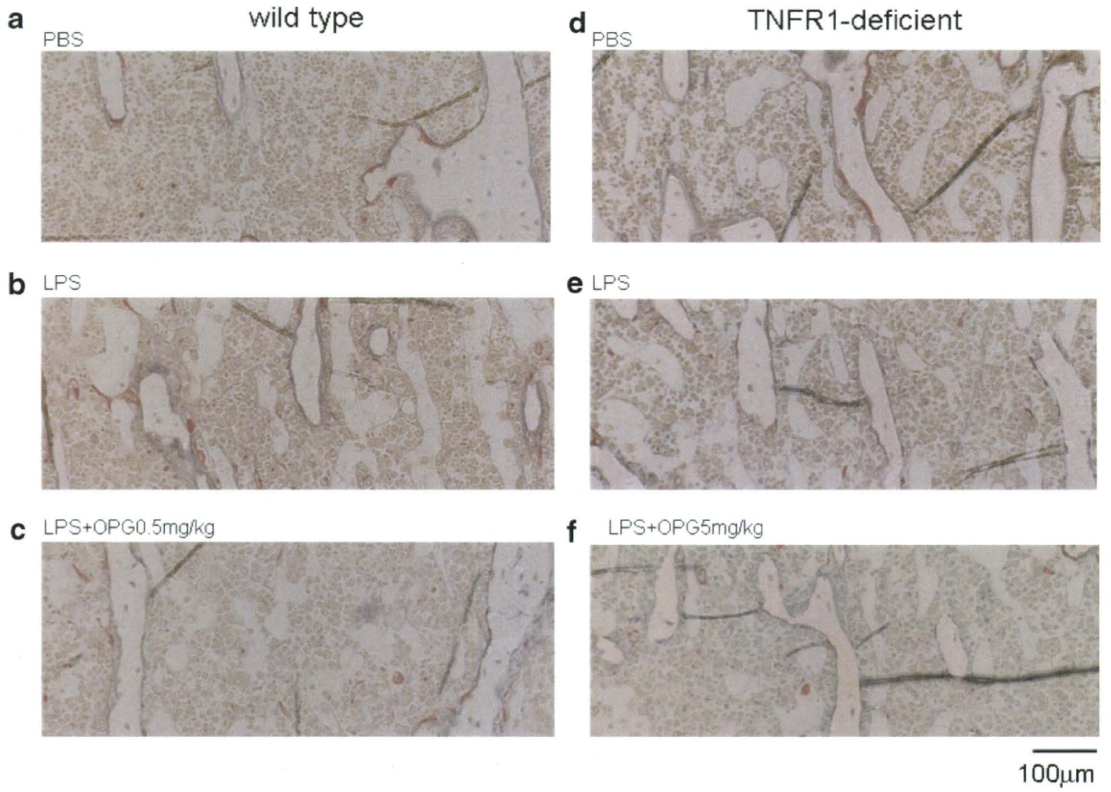

Figure 2. LPS injection induced high turnover osteopenia in wild-type mice and low turnover osteopenia in TNFR1−/− mice. Sections of tibiae from wild-type (a–c) and TNFR1−/− (d–f) mice were stained for TRAP activity (stained red) and ALP activity (stained purple). Osteoclast number was increased only in LPS-injected wild-type mice (b). ALP-positive area was also increased in LPS-treated wild-type mice (b), but decreased in LPS-treated TNFR1−/− mice (e, f). Both Oc.S/BS and N.Oc/BS were significantly increased in LPS-treated wild-type mice (g, h). OPG treatment suppressed the LPS-induced osteoclastogenesis in a dose-dependent manner (g, h). LPS or OPG had little effect on N.Oc/BS and Oc.S/BS in TNFR1−/− mice (j, k). Urinary deoxypyridinoline was increased on the day after LPS injection in wild-type mice only (i, l). Bars, ±SD. Asterisk indicates statistically significant difference ($p < 0.05$).